THE SEA: THE SCIENCE OF OCEAN PREDICTION
*Journal of Marine Research, 75,* 103–159, 2017

# From weather to ocean predictions: an historical viewpoint

**by Nadia Pinardi[1,2], L. Cavaleri[3], G. Coppini[4], P. De Mey[5], C. Fratianni[6], J. Huthnance[7], P. F. J. Lermusiaux[8], A. Navarra[4], R. Preller[9], and S. Tibaldi[4]**

ABSTRACT

This paper reviews the historical development of concepts and practices in the science of ocean predictions. It begins with meteorology, which conducted the first forecasting experiment in 1950, followed by wind waves, and continuing with tidal and storm surge predictions to arrive at the first successful ocean mesoscale forecast in 1983. The work of Professor A. R. Robinson of Harvard University, who produced the first mesoscale ocean predictions for the deep ocean regions is documented for the first time. The scientific and technological developments that made accurate ocean predictions possible are linked with the gradual understanding of the importance of the oceanic mesoscales and their inclusion in the numerical models. Ocean forecasting developed first at the regional level, due to the relatively low computational requirements, but by the end of the 1990s, it was possible to produce global ocean uncoupled forecasts and coupled ocean-atmosphere seasonal forecasts.

*Keywords:* atmospheric predictions, wave and sea level predictions, mesoscale predictions

## 1. Introduction

Until the first decades of the nineteenth century, oceanography was governed by the need to explore unknown regions of the world's oceans and collect basic scientific observations that described the structure of currents and the associated processes. This naturalistic approach was characteristic of astronomy, meteorology and other earth sciences in their early stages of development. In oceanography, this descriptive approach continued substantially unchanged until the publication of "The Oceans" by Sverdrup, Johnson, and Fleming in 1942 (Sverdrup et al. 1942). This treatise on modern interdisciplinary oceanography

1. Department of Physics and Astronomy, University of Bologna, Viale B. Pichat 6/2, 40127 Bologna Italy
2. Corresponding author: ***e-mail: nadia.pinardi@unibo.it***
3. CNR-Istituto di Scienze Marine, Venice, Italy
4. Centro EuroMediterraneo sui Cambiamenti Climatici, Lecce, Italy
5. LEGOS, Toulouse, France
6. Istituto Nazionale di Geofisica e Vulcanologia, Bologna, Italy
7. Proudman Oceanographic Laboratory, Bidslon Observatory, Birkenhead, Merseyside, United Kingdom
8. Department of Mechanical Engineering, Massachusetts Institute of Technology, Cambridge, MA 02139, USA
9. Naval Research Laboratory, Stennis Space Center, Mississippi, USA

connected theory and experimental data in an unprecedented synthesis of ocean thermodynamics, dynamics, chemistry, biology, and geology. It turned oceanography into a new branch of science in which quantitative and mathematical theories were used to explain the properties of oceans, from physics to ecosystem variables. Even with such a formidable step in marine knowledge, it was not until much later that large-scale ocean prediction was recognized as a fundamental issue in oceanography, similar to the developments in meteorology and hydrology.

Quantitative predictions require precise knowledge of the physical principles responsible for the evolution of a flow field. Until the nineteenth century, physics focused on the discovery of new fundamental laws that describe the structure of the universe, its basic forces, and the basic constituents of mass. The theory of fluids constitutes the basic framework for meteorology, oceanography, and hydrology; it was developed at the same time in engineering and physical sciences because, given the extremely large spectrum of scales (from $10^{-6}$ to $10^4$ km) contained in the fundamental equations, both basic understanding and practical solutions are required.

The dynamic equations had already been written by Navier (1822) and Stokes (1848) but nobody attempted to solve them as a time-dependent problem before the 20th century. By adding thermodynamics, the basic prognostic laws of fluids can be synthetically written as:

$$\frac{\partial \mathbf{x}}{\partial t} = F(\mathbf{x}, t) + \Lambda(\mathbf{x}, t) \tag{1}$$

where $\mathbf{x} = [u, v, w, p, T, S, q]$ is the vector containing the basic state variables that describe the fluid, i.e., the three components of velocity $(u, v, w)$, pressure $p$, temperature $T$, salinity $S$ for ocean or specific humidity $q$ for the atmosphere. Here $F$ contains the advection, the rotation, the gravity, and the internal, resolved forces per unit volume, while $\Lambda$ encompasses the turbulent and molecular stresses. Adding the diagnostic equation of state for $\rho$ for the ocean and atmosphere, there are seven unknowns and seven equations. "*Predictions*" are the result of solving the time evolution of the system when both the initial conditions and the boundary conditions in the three-dimensional (3D) space are known, a process known as "*integration*." These equations are nonlinear and their associated initial boundary value problem is ill-posed with any specification of local, pointwise boundary conditions (Oliger and Sundström 1978; Temam and Tribbia 2003).

Notwithstanding this basic mathematical problem, Bjerknes (1904, 1914) defined a practical way to solve these equations, coining the name "*weather* and *hydrology predictions*." In these papers, Bjerknes described a method that could solve equations (1) at least for a finite, and, at first, short, amount of time. He defined two factors that were necessary to make weather and hydrology predictions a reality: (1) knowledge of the initial conditions should be as accurate as possible, and (2) the development of an accurate predictive model. The latter consisted of discretizing (1) and using numerical methods to solve for the time derivative, as was later attempted in the pioneering work of Richardson (1922). We had to wait until after World War II to see numerical weather predictions become operational, strongly supported by the newly born aviation sector.

Ocean forecasts for practical applications need to consider sea level, wave, current, temperature, and salinity predictions simultaneously, to mention just the physical components. However, solving all of these variables simultaneously was too difficult because of the limited knowledge of processes and the computational requirements. Knowing that the energy containing variability peaks at different time scales for different state variables and that spectral gaps exist, a practical framework for ocean predictions emerged: the dynamic evolution of the sea level was decoupled from the evolution of surface waves, and short sea level variability was decoupled from currents, temperature and salinity predictions.

Ocean forecasts were first developed for wind waves. In 1947, Sverdrup and Munk published a technical note (Sverdrup and Munk 1947) that described the theory and the practical methodology for surface wind wave forecasting. The first wind wave forecast was achieved in 1942–1943 and was used to support the allied forces in Africa and Europe (Munk 2002). Given the rather easy observational requirements for surface wind waves, this development did not spur the same endeavor for ocean currents, with their much greater observational requirements. Deterministic wave predictions reached maturity in the mid-1980s with the implementation of numerical wave models for the specific case of surface wind waves.

Sea level forecasting was the second ocean phenomenon to achieve forecasting capability, because reasonable prediction accuracy could be achieved using only astronomical tidal forcing, winds, and atmospheric pressure. In addition, Flather and Davies (1976) used shallow water equations, an approximate set of calculations that could be solved with robust numerical methods.

We had to wait until 1983 for the first successful forecast of 3D ocean currents, produced by Allan R. Robinson's group at Harvard University (Robinson et al. 1984). There were extensive requirements for estimating the initial ocean condition fields and data had to be collected specifically for this purpose. A precise experimental survey was planned that would collect data in a short time for a relevant spatial domain extension, approximately $100 \times 100$ km$^2$. Successful two-week ocean "weather" predictions were produced for the California ocean current system, representing the equivalent of the meteorological weather prediction over the US produced by Charney, Fjortoff, and Von Neuman at Princeton University in 1950.

In this chapter, our approach is to show the historical development of prediction capabilities starting with meteorology, ocean waves, sea level, and ocean currents from short to longer time scales, and from sub-regional to global scales. Most of these developments involved the simplification of fundamental equations (1) to achieve predictive capabilities at the selected space and time scales, thus making it practical to solve problems with the numerical computer resources available over the past 60 years.

Today, the various predictable ocean phenomena are beginning to be combined in a unique framework that considers waves, currents, sea ice, atmosphere, and hydrology together. In terms of ocean ecosystems, marine environmental predictions started to become practical at the beginning of the twenty-first century (Pinardi and Woods 2002). The approach couples the physical predictive equations (1) with biogeochemical semi-empirical predictive equations that describe the rate of change of phytoplankton biomass, particulates and dissolved organic and inorganic chemical families (Vichi et al. 2007; Lazzari et al. 2010). The accuracy of biochemical predictions should improve as the observational capacity increases over the next few decades.

The paper begins with a description of meteorological predictions in Section 2, continues with wave predictions in Section 3 and sea-level tide, and storm surge predictions in Section 4. The first mesoscale predictions are introduced in Section 5, while regional and relocatable forecasts are described in Section 6. A short overview of global scale forecasting is given in Section 7 and a discussion concludes the paper.

## 2. Setting the scene: meteorological predictions

Why should we discuss weather forecasting in a volume on the science of ocean prediction? The answer is that oceanography can benefit from meteorology's longer tradition and experience of operational forecasting. Similarly, following the lead of the global meteorological system, a wide variety of practical applications in a broad spectrum of areas could benefit from regular, daily global operational ocean forecasts, like early warning for storm surges, optimal ship routing, search and rescue, oil platform operations, marine ecosystem health, fisheries, optimal offshore wind energy and mariculture siting, to mention only few. Even numerical weather prediction itself can (and does) take great advantage from good ocean wave and sea surface temperature forecasts, since what happens at the ocean-atmosphere interface is important for meteorology. Indeed, over the past 60 years or so, we have become accustomed to the ever-increasing accuracy and reliability of the forecast products produced by global operational meteorology (see, for example, Fig. 1 for the evolution of the European Centre for Medium-Range Weather Forecast's (ECMWF) operational medium-range forecast performance scores during the last 35 years) and, therefore, to their practical usefulness. However, these improvements were the product of intense scientific and technical development efforts.

### *a. The early days*

In fact, although meteorology is a comparatively young science, weather forecasting is an even younger scientific endeavor. The first seed of the concept of weather forecasting as a physical problem that could be expressed with equations, and was in turn amenable to mathematical solutions, dates back to the American meteorologist Cleveland Abbe at the turn of the nineteenth century (Abbe 1901). It is, however, customary to date the birth of hard-science meteorology to the pioneering work of Vilhelm F. K. Bjerknes, who in 1914 (Bjerknes 1914) proposed the first set of governing equations for the evolution of the atmospheric state, based on the main dynamic and thermodynamic conservation laws of

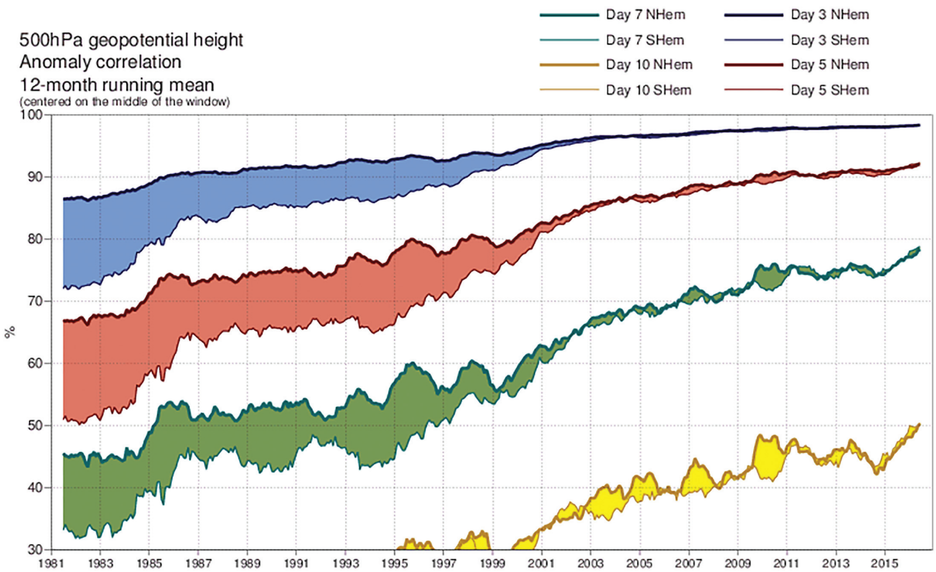


Figure 1. Anomaly correlation coefficient of 500 hPa geopotential height for day 3, day 5, day 7 and day 10 forecasts. Thick lines: Northern Hemisphere, thin lines: Southern Hemisphere. In color the progressively diminishing difference between the two hemispheres is noted. (Source: http://www.ecmwf.int/en/forecasts/charts/medium/anomaly-correlation-ecmwf-500hpa-height-forecasts?time=2017011100).

mass and energy and on the equation of state for gases. In fact, he had anticipated the basic principles of his program in 1904 (Bjerknes 1904), when he went as far as declaring that seven equations for the seven canonical variables ($p$, $T$, $u$, $v$, $w$, $q$, and $\rho$, i.e., atmospheric pressure, temperature, 3D velocity ($u$, $v$, $w$), moisture, and density) were sufficient to determine future states of the atmosphere given the initial conditions. He was perfectly aware that solving the set of differential equations analytically was impossible, and repeatedly stated that a graphically or numerically approximate solution would have to suffice. However, he never made a real practical attempt to do so.

The first practical attempt was in fact made by Lewis Fry Richardson, a nurse and ambulance driver during the First World War and a conscientious objector who refused to fight actively. Richardson was prepared to spend endless hours performing the necessary mathematical computations. In the complete account of his attempt, published in 1922, he acknowledged the profound influence of Bjerknes' work on his choice of prognostic equations (Richardson 1922). Richardson first of all corrected Bjerknes' set of equations by simplifying the thermodynamics and by adding mass conservation for atmospheric moisture, thereby obtaining a closed set of seven equations for the seven variables. However, he was also very familiar with graphical and numerical methods of obtaining approximate solutions for differential equations. His attempt was based on the right set of equations and the correct sequence of operations, which even today form the basis of operational numerical weather predictions, including a complete set of centered finite-difference schemes by which he replaced differential equations with difference equations. Nevertheless, it turned out to be a complete failure.

There were a number of reasons for his failure. In the first place, Richardson added several additional terms to the original equations proposed by Bjerknes to account for minor effects that were later found to be negligible. There was a far more fundamental problem, however, and again it had to do with the choice of equations to be solved. Even if Richardson had chosen to use the correct set of seven equations with no further unnecessary complications, he would have failed anyway, since he was unaware of the existence of numerical stability criteria, both linear and nonlinear, that must be satisfied to obtain a meaningful solution. The linear stability criterion, the so-called CFL criterion (after Richard Courant, Kurt Friedrichs and Hans Lewy, formulated later, in 1928, and translated in Courant et al. (1967)), requires that the ratio of the grid size and the time step be larger than the speed of the fastest air parcel or wave motion described by the equations. Because Richardson's (and Bjerknes') dynamical equations were essentially Euler's equations for a compressible fluid on a rotating earth, both gravity and sound waves were possible solutions. This meant that the fastest speed was the speed of sound, which in turn rendered the choice of grid size and time step impossible to tackle using hand computations. As for nonlinear stability problems, Richardson was unaware of energy and enstrophy cascades and of the need to remove cascaded energy from the smallest resolved scales by adding dissipative terms, although he spent a great deal of effort studying turbulence and how it should be taken into account in the forecasting scheme.

The failure took the form of a six-hour forecast of surface pressure for two grid boxes over the British Isles for May 20, 1910. One grid box indicated a pressure change of 145 hPa (mbar at the time) compared with an observed change of less than 1 hPa, and all after 6 weeks of arithmetical computations by hand! One could also note that, even if the computations had yielded a reasonable output, producing a 12-hour forecast for a few hundred grid boxes would have taken an impractical 10 years. In fact, Richardson had already considered this problem and proposed to employ a small army of human "computers," arranging them in a grid-like assembly, positioned next to each other in the Royal Albert Hall in South Kensington, a space that can seat more than 5000 people!

It took 24 years, another world war and the contributions of outstanding meteorologists and mathematicians, including Carl-Gustaf Rossby and Alan Turing, before John von Neumann—probably one of the most eclectic geniuses of his time—became convinced that the problem of weather forecasting was the very application he needed to convince the United States government to invest in the development of fast, programmable computing machines. This was 1946, yet even von Neumann and his Meteorology Project, housed at the Institute for Advanced Studies in Princeton, made little progress until 1948, when Jule Charney joined the team as director of the project. He then called on Arnt Eliassen from Norway to help him.

Charney developed the quasigeostrophic approximation (Charney 1948) and produced a prognostic equivalent barotropic vorticity equation that filtered out all fast-traveling, nonmeteorological gravity waves, allowing the computational power available at the time (von Neumann's ENIAC) to produce a usable numerical forecast (Charney et al. 1950; Charney 1955). It was March 1950. Another two years later, in 1952, the essential contribution of Norman Phillips (Phillips 1951) was a linearized, baroclinic, two-layer model that was capable of equaling—, and often surpassing, —the quality of subjective, hand-drawn forecast maps produced daily in the forecasting rooms of the world's top weather services. It was the dawn of operational numerical weather prediction. See Platzman (1979), Lynch (2008), and Nebeker (1995) for descriptions of those early experiments.

*b. Modern numerical weather prediction*

With ever-increasing computing power at the disposal of meteorology, and the growing ability of meteorological modelers to extract information from the global observational network (we return to the problem of data assimilation later), the need for smaller and smaller scales was becoming a pressing problem, requiring the abandonment of some of those equation-filtering techniques that had allowed the first numerical forecasts. From the late 1950s to the mid-1960s, the filtered models were being replaced with models based on the so-called primitive equations. These were practically the same equations that Bjerknes and Richardson believed could be used to forecast the weather, except for the hydrostatic approximation in the vertical momentum equation to filter out vertically traveling sound waves (for a brief discussion on the need to filter out meteorological "noise," see, e.g., Holton and Hakim (2012), sect. 13.2) and the introduction of a Laplacian-based diffusive term in the two horizontal momentum equations to control nonlinear instability. A great cycle had come to completion, and the intuition and dream of Bjerknes and Richardson had come true. The growing availability of electronic computing power, together with the fantastic development of theoretical and applied meteorology and meteorological engineering, had made the dream possible.

After that first forecast of 1950, it took another 27 years of continuous numerical model development, carried out in the main operational weather centers and research institutions of the world, before the newly born European Centre for Medium-Range Weather Forecasts (ECMWF), a European intergovernmental organization founded and based in Reading, UK, under the masterly guidance of Aksel Wiin-Nielsen produced its first operational medium-range forecast in June 1979. The prototype model had been written in less than two years on the basis of recent developments and improvements, and thanks to the intellectually and practically generous contribution of the Geophysical Fluid Dynamics Laboratory in Princeton, which had just shown the feasibility of medium-range forecasts (Miyakoda et al. 1969, 1972). Modern, contemporary European numerical weather prediction was born and, almost immediately, ECMWF forecasts became the best in the world for analysis and forecast quality. The center's leadership continues to this time (Woods 2006).

Those 27 years, between 1950 and 1977, were dense in developments and discoveries, and the birth of the ECMWF also coincided with the realization of what was called the largest scientific experiment ever conducted; the First GARP Global Experiment (FGGE). GARP (Global Atmospheric Research Programme, which began in the second half of the 1960s) was the most important research effort of the World Weather Watch (WWW), itself the core development program of WMO, or World Meteorological Organisation (a UN Meteorological Agency). The FGGE, which took place in 1978–79, was a global observation experiment with the main aim of providing global datasets to initialize and verify the capability of atmospheric global models to represent and forecast atmospheric behavior. It was a truly international experiment that was carefully planned, prepared, and conducted. It lasted 12 months and entailed launching, flying, and sailing innumerable extra radiosondes, drifting ocean buoys, ships and aircrafts, and even an extra satellite: NIMBUS-7. The main objective of FGGE was indeed of particular relevance to our brief historical excursus. As Paul Edwards states in “A Vast Machine” (Edwards 2010), the FGGE global dataset gave an essential push to the possibility of making experiments with models to better understand the real world, and improved the realism and ability of models to represent the real atmosphere. This was probably the official birth of numerical experimentation, which is, today still one of the pillars of research and development in the science of Numerical Weather Prediction. Numerical experimentation is based on the use of modeling as the substitute for that global earth weather and climate laboratory that we will never have at a 1:1 scale.

### c. *The role of observational data and the global infrastructure*

In this short account of the development of numerical weather prediction, we have not forgotten to describe the central role of observational data in operational numerical prediction. Another reason for Richardson’s failure was the problem of knowing with sufficient accuracy the state of the atmosphere at a single instant in time, or, more technically, having sufficiently good initial conditions. Two essential ingredients are required to produce a good instantaneous snapshot of the state of the atmosphere: enough accurate and synoptic observational data for all of the important variables and good physically based mathematical methods to blend these data into a consistent, 3D picture as accurately as possible. Neither of these two ingredients was available to Bjerknes or Richardson, and they remained operationally unavailable for a very long time.

The problem of producing even a basic picture of the 3D state of the atmosphere at a given instant remained essentially intractable until after the Second World War, with the advent of good radio communication technology and good aviation transport. The development of commercial and military aviation facilities made 3D exploration of the atmosphere at the same time possible and necessary. The FGGE and the global meteorological observation system it gave birth to provided the rest.

The problem of meteorological data analysis was first conceived as a classic two-dimensional (2D) mathematical interpolation problem: how to obtain the values of all directly observed atmospheric variables at sea level or at a given constant pressure level, and on a regular mesh of grid-points covering the area of interest (the Northern Hemisphere at mid and high latitudes at first, but very soon the entire globe) given the measured values in an extremely irregular and inhomogeneous set of observation points. That is, all synoptic weather stations on land and on ships, taking measurements every few hours, and all radiosonde stations launching weather balloons once or twice a day. Meteorologists usually referred to this 2D interpolation problem as the problem of "objective analysis" (Gilchrist and Cressman 1954). This was in opposition to the highly professional (and unfortunately fairly subjective) skill of hand-drawing isopleths of mean sea level pressure or geopotential height at constant pressure levels on the synoptic charts, on the basis of which all national weather services formulated equally subjective short-range forecasts twice a day. It was not until the early 1960s that computer-produced, objective analyses started competing successfully with human-produced, hand-drawn synoptic charts, and gradually put them out of business by replacing them altogether. This was not only because their quality was initially comparable and soon became better and more homogeneous in time and space, but also because the rapidly decreasing cost of computer power meant the computer-produced analyses were cheaper (Edwards 2010).

The 1960s were a truly revolutionary period for operational meteorology, with the combined appearance on the operational scene of digital computers, automatic objective analysis techniques, numerical weather predictions based on mathematical models, meteorological satellites and the first weather radars. All of these data were internationally exchanged at the fastest transfer speed possible at the time by the World Weather Watch, overseen and coordinated by an ad hoc UN Agency, the World Meteorological Organization. All of these systems together gave rise to the "Global Weather Information Infrastructure," the realization of which made the birth of modern global meteorology possible (Edwards 2010).

### *d. The ever increasing role of remote sensing*

Meteorological satellites in particular represented an essential breakthrough, allowing the bench forecaster the capability of actually "seeing" the state of the atmosphere he had to analyze and whose developments he had to predict. Very soon, satellites started producing not only nice (and very useful in forecasting practice) pictures of the clouds in the visible and infrared bands, but also quantitative radiances from which atmospheric vertical temperature profiles could be derived (retrieved, in jargon). In fact, they started producing these data in such great quantities that digital data transfer rates and computational power were hardly capable to cope with such a wealth of data. This intense production of information by satellite continues to this day.

The first approach was to use these "retrieved" temperature profiles as "satellite vertical soundings," a sort of radiosonde temperature profile taken from above instead of below, sometimes together with the wind estimates derived from cloud displacements, and to use them in well established objective analysis algorithms (Gandin 1965) to compute the current state of the atmosphere. In the meantime, the very primitive, simple, pure, interpolation-based objective analysis systems developed first into optimum interpolation methods and then into much more sophisticated "data assimilation systems." Using these systems, observed data were blended, usually at fixed moments in time, e.g., four times a day, into "first guess fields" provided by very short-range (6-hour) global forecasts, so that information from data-dense areas could be *advected*, that is, propagated, into data-sparse areas of the globe to produce global atmospheric analyses with a reasonably uniform quality (Lorenc 1986).

However, complications arose. By the mid-1980s, meteorologists were already aware of the annoying truth that such comparatively large amounts of satellite-retrieved temperature data, although extremely useful over very large data-void areas such as the Southern Oceans, were not particularly useful over data-dense areas of the Northern Hemisphere. There, numerical forecasts were sometimes better if retrieved satellite temperatures were left out altogether (Uppala et al. 1984). This trying state of affairs indicated that the information contained in satellite data was not being used in the best possible way and that alternative data analysis methods were needed. This was one of the most important motivations for the development of variational data assimilation techniques, a mathematically much more sophisticated technique of extracting information from observed data (Talagrand 2003).

The basic idea is to combine very short-range model forecast (the first guess) with observational data in a mathematically optimal way (by minimizing a so-called cost function, representing the distance between analysis and the unknown truth), to provide the best possible estimate of the atmospheric state. A great step forward was represented by the way in which the first guess was generated. Rather than preprocessing observational data to produce the atmospheric variables that the first guess was providing (the prognostic model variables, e.g., temperature), the model first guess variables had to be processed in turn, so to produce, via suitable observation operators, the quantities that observation instruments were directly measuring. In the case of satellite-borne radiometer data, for example, rather than retrieving temperatures from radiance data and then using retrieved temperatures, radiances had to be produced from model temperatures to be compared immediately with observed satellite radiances. The same, of course, would have occurred in the following years for all other observational data not providing directly the prognostic model variables, for example, radar backscatter (ground-based or satellite-borne) or GPS-derived optical depths. This substantial, philosophical change in approach allowed useful meteorological information to be extracted from unconventional observation in a much better, more efficient way (Daley 1991; Rodgers 2000).

Thus, in the very late 1980s, more than 20 years after their appearance on the meteorological scene, satellite data started to become one of the most important sources of quantitative information for producing daily, operational, digitally produced, numerical weather forecasts. Meteorology had entered a new era, the era of remote sensing.

### *e. Nowadays: new, more ambitious techniques*

The extraordinary increase in digital computing power at the disposal of operational meteorology (see Fig. 2) meant that additional important model components, such as sea wave modeling and even simple ocean models would soon become available. It also allowed the exploration of other avenues, such as limited area modeling, ensemble prediction techniques and the extension of forecasts beyond the medium range, up to the seasonal scale,

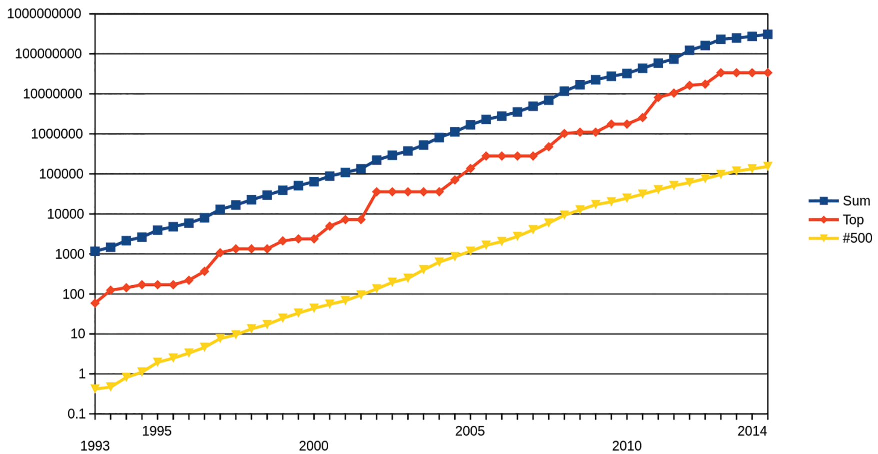


Figure 2. The exponentially rapid growth of supercomputers during the last 23 years, based on data from www.top500.org. The logarithmic y-axis shows performance in GFLOPS. Blue line: combined performance of 500 largest supercomputers. Red line: fastest supercomputers. Yellow line: supercomputers on 500th place. By AI.Graphic - Own work, CC BY-SA 3.0 (https://commons.wikimedia.org/w/index.php?curid=33540287). Meteorology has been estimated, during the 1970s, 1980s, and 1990s, to be second only to the development of nuclear weapons as the most demanding client of high performance supercomputing power. (Source: https://en.wikipedia.org/wiki/History_of_supercomputing).

i.e., beyond the deterministic predictability limits (for a review of atmospheric predictability, see, e.g., Palmer and Hagedorn (2006)). Limited area modeling enabled the production of very high spatial resolution models for limited portions of the globe—where detailed (mostly short-range) forecasts were particularly useful—by "nesting" high-resolution models in coarser global models.

Over the past 25 years, ensemble prediction systems have made the dream of quantitative, physically based, probabilistic forecasts a reality (Epstein 1969; Murphy 1998). These systems make it possible for numerical weather prediction-based forecasts to manage the unavoidable uncertainty, which increases over the forecast period due to the combination of errors in the initial conditions, errors in the formulation and solution methods of the evolution equations and the chaotic behavior of the atmosphere over the timescale of a few days to a few weeks (for chaotic atmospheric behavior on weather and climate timescales, see, for example, the chapters by Lorenz and Palmer in Palmer and Hagedorn's Predictability of Weather and Climate 2006).

The basic idea is to "run" the model not just once, as in the usual "deterministic" mode, but several times, thereby producing a high number (order 50–100) of realizations of the same forecast (the "ensemble"). This action is done by appropriately perturbing, for example, the initial condition fields, and (as a result of more recent development) by also perturbing model tunable parameters as the integration proceeds. The frequency of occurrence of a given phenomenon among ensemble members, e.g., overcoming a given threshold value

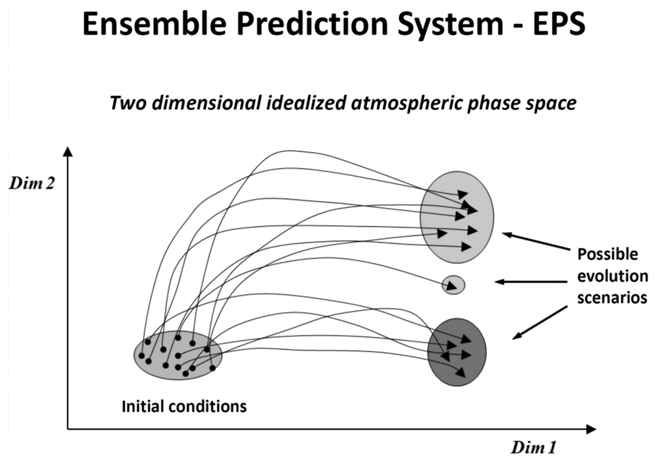


Figure 3. Schematic representation of an Ensemble Prediction System in an idealized atmospheric phase space. Starting from approximately equiprobable initial conditions, the model evolves in time along slightly different trajectories. In this space the different final solutions are clustered in a few different scenarios, whose population can be associated to their *a posteriori* probability of occurrence.

for a given model variable, be it temperature or precipitation or any other, will then provide an *a posteriori* estimate of the probability of occurrence of the phenomenon itself (see Fig. 3). The ensemble technique was initially explored in the late 1970s by Tony Hollingsworth at ECMWF, as a specific application of the Monte Carlo technique to meteorological forecasting. Hollingsworth's first attempt was, however, disappointing (Hollingsworth 1980) but the technique was pursued further and progressively developed both in Europe and in the United States until it became, during the past 25 years, operational in all major prediction centres in the world. It is used not only for short- and medium-range forecasts, but also for extended-range up to seasonal and decadal predictions (Balmaseda, 2017, this volume), and seems to be an extremely promising technique for the ocean as well. Meteorological predictions have gone a long way since the early days of Bjerknes and Richardsons dreams and intuitions. But let us recollect that already in 1970, B. J. Mason (Mason 1970) anticipated that oceanography would follow meteorology along similar operational lines before the end of the 20th century. We are well into the 21st century and ocean observing systems have seen fantastic developments. It is therefore time that numerical ocean predictions make their way into everyday operational practice.

## 3. Wave predictions

### *a. A look at the past*

Waves are the most evident ocean phenomena affecting human activities at sea. For a long time, the safety of a vessel and of the persons and goods on board relied on the experience of the vessel captain, experience that was distributed little by little around the world.

While direct experience soon made it clear that wind was the cause of large ocean waves, the mechanism by which energy and momentum were transferred from the atmosphere to the ocean remained elusive for a long time. It may not be surprising, therefore, that no solid theory was developed for the generation of waves by winds, notwithstanding the advances in fluid dynamics in the nineteenth century. The first attempt that can be considered as such was by Jeffreys (1925), who tried to estimate the force exerted by wind on the back-facing side of the wave. This rather intuitive approach did not manage to account for the basic energy of waves, and the problem was left aside for several decades.

Then, during the Second World War, the problem was put abruptly on the table when it became clear that military operations depended on the transfer of troops from ship to shore via the dangerous surf zone. The U. S. Navy put the problem in the hands of Harald Sverdrup, director of the Scripps Institution of Oceanography at La Jolla, California. Sverdrup and his student, Walter Munk, using their knowledge, intuition and a limited amount of data, managed the following year to provide a wave diagram simple enough to be used by any interested person (Sverdrup and Munk (1947); Figure 4). Given the wind speed, the fetch length, and the number of hours the wind had been blowing, the diagram provides the significant wave height and period of the local waves. The diagram was so good and easy to use that it remained in practical use for several decades, until deterministic wave forecasts became feasible.

The main difficulty was the apparently random nature of the sea surface, where, with the exception of the dominant waves, the main characteristic seems to be the lack of order. The solution was provided by Pierson and Marks (1952), who suggested, on the basis of a parallelism with light, that a sea surface can be conceived as the superposition of a sufficient number of regular unidirectional sinusoidal waves with different frequencies (hence period and length), heights and directions. This spectral approach hugely simplified the problem because it was then possible, assuming the superposition of effects, to evaluate the wind input to the single components. This prompted physicists to rapidly provide two different but complementary mechanisms for the generation of waves by wind. The first approach, proposed by Phillips (1957), examined atmospheric pressure oscillations, while Miles (1957) relied on the deformation of the wind field running on top and adapting itself to the shape of the surface waves. The Miles physical process requires an existing undulation on the surface, which was provided by the Phillips mechanism, starting from the ideal flat surface. In the meantime, Gelci et al. (1957) wrote the energy balance equation that dynamically regulates the evolution of the single wave component.

This understanding made it possible to evaluate the wave conditions when wind and bathymetry information was available. The first numerical model based on the spectral decomposition of the sea state was produced in 1956 by the French Weather Service, and focused on the North Atlantic (Gelci et al. 1957). In the 1970s, the first operational, hemispheric wave model was running at the Fleet Numerical Oceanography Center, Monterey, California (Cardone et al. 1975); it was called the Spectral Ocean Wave Model, or SOWM.

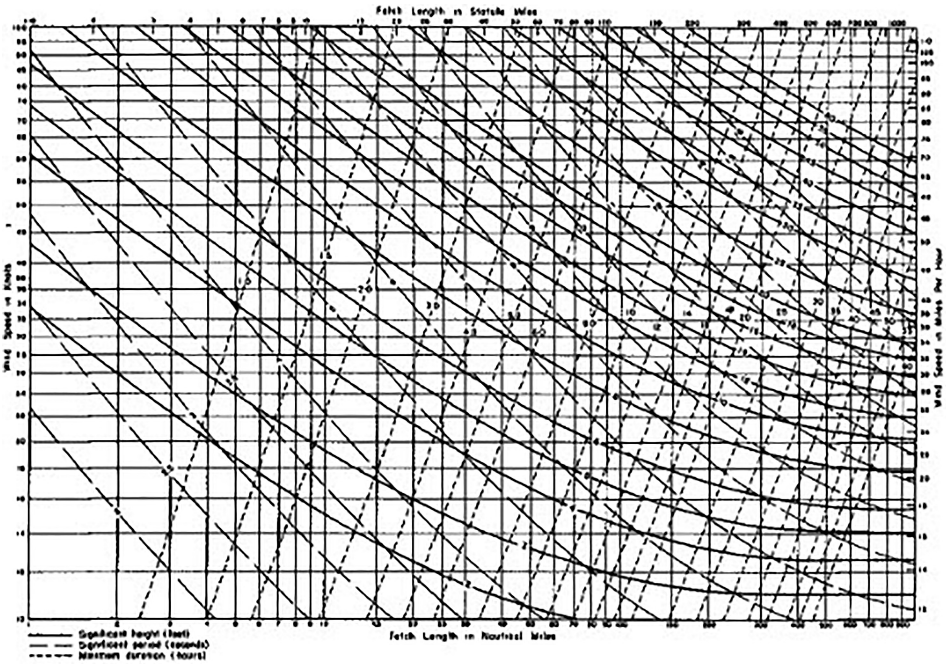


Figure 4. The original diagram of Sverdrup-Munk for estimating significant wave height (units foot, thick continuous lines) and significant period (units seconds, dashed lines) as a function of wind speed (units knots, y-axis), fetch (units miles, x-axis), and duration (units hour, short diagonal dash lines).

In 1985, SOWM was replaced by a global version, called GSOWM, that extended from 77.5N to 72.5S and ran on a .25-degree grid (Rogers et al. 2014).

The first approaches were rather empirical for the shape of the spectra and the limits of the wave growth. It was also clear that the spectral approach implicitly relied on the hypothesis of linearity. This limitation was removed by Hasselmann (1962), who provided the theoretical background for evaluation of nonlinear wave effects. The nonlinear wave interactions were proved in the JONSWAP experiment (Hasselmann et al. 1973). However, calculation of the corresponding energy exchanges among the various wave components was then, and still is, beyond any practical computational feasibility. Therefore, in the 1970s and early 1980s, a number of pre-calculated spectral shapes were made available for use in the numerical calculations, such as the North Atlantic wave model of Ewing (1971). Other examples followed, but still with the limitations imposed by the evaluation of the nonlinear interactions. Somehow overestimating the role of nonlinear interactions in the ocean, Hasselmann et al. (1976) suggested a model fully based on them, e.g., with a practically instantaneous alignment of waves with wind direction. This model was then partially modified in the mixed wind sea-swell approach by Gunther et al. (1979).

The launch of the ERS-1 satellite, offering the possibility of using Synthetic Aperture Radar to measure the 2-D wave spectra, prompted Hasselmann et al. (1985) to devise the discrete interaction approximation, a simplified but still effective way to evaluate nonlinear wave interactions. This innovation opened the way to the so-called third-generation wave models, the main characteristics of which were the full evaluation of the elements of the energy balance equation on purely physical terms. The first example was WAM ("WAM Group," 1988; Komen et al. 1996), soon followed by WAVEWATCH (Tolman 1997) and SWAN (Booij et al. 1999), the last of which was mainly suitable for shallow water applications. These three models, all open source, together with the commercial version MIKE21 of DHI, and the less well-known model by Abdalla (Abdalla and Özhan 1993), provided the general wave forecast modeling framework.

A more complete reference and description of the present approaches in wind wave modeling and connected problems are given by Babanin et al. (2017, this volume).

*b. A look at today*

Nowadays, the physics of wind wave generation is assumed to be well known. The three fundamental processes, generation by wind, dissipation by white-capping and nonlinear interactions, have their own formulations and, when coupled with sophisticated numerical schemes, lead to accurate results (Janssen 2008). Predicting wave conditions up to several days in advance for any part of the globe is now possible. The statistics of the major meteorological centers speak for themselves with an average worldwide bias of a few centimeters or less for the significant wave height. We report the statistics of the ECMWF (Reading, UK) in Figure 5.

Such accurate forecasts stem from a few basic scientific and technological advances. Ever-increasing computer power has allowed a dramatic increase in the resolution of both meteorological and wave models. Physics has improved and has been incorporated in the equations up to second-order processes. A typical example is the attenuation of swell along the extended trajectories in the ocean due to the small, but appreciable with time and distance, transfer of energy and momentum to the atmosphere (see Ardhuin et al. 2010). More processes appear in coastal and shallow waters, and here too the use of nested and unstructured high-resolution models, and possibly nonlinear equations (e.g., Boussinesq and mild slope equations; see Lamb 1932), has led to results that satisfy most practical needs. Another area of development is probabilistic forecasts of particularly large (freak) single waves in a storm.

A key idea behind the recent, and no doubt future, improvements is the coupling between ocean, waves, and the atmosphere. By 1991, Janssen (1991) had already shown how the wave field information was crucial for improving meteorological forecasts because of the different surface friction felt, and momentum transfer, by the atmosphere. Wave breaking is crucial in establishing wind-driven currents (McWilliams and Restrepo 1999). Conversely, Gallet and Young (2014) showed how a long distance swell is affected by ocean currents. This interaction is what determines whether the swell is blocked by Antarctic ice. The

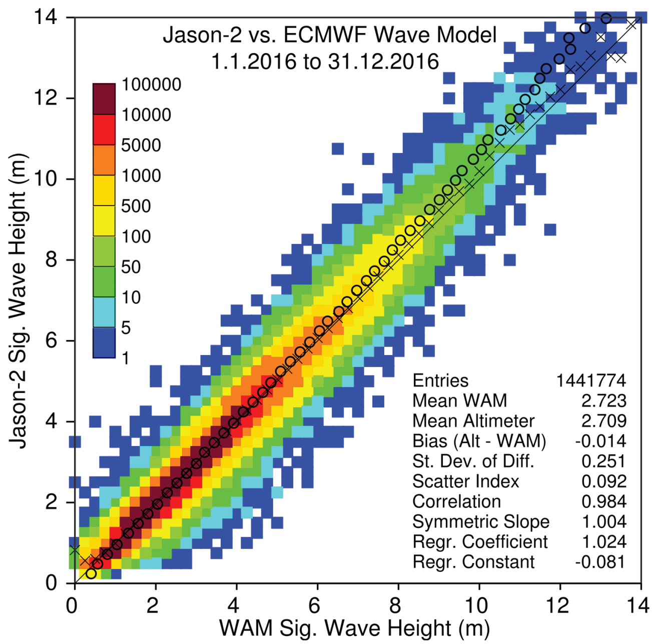


Figure 5. Intercomparison between the ECMWF model significant wave heights and the corresponding altimeter measured values. Data for year 2016 of Jason-2 altimeter.

classical historic example by (Snodgrass et al. 1966) well illustrated how Indian Ocean storms may send swell toward California. As a final example, Cavaleri et al. (2017), using the latest operational version of the fully coupled ECMWF modeling system, succeeded in explaining the iconic, so-called Draupner wave that hit the Draupner measuring platform in the North Sea on January 1, 1995.

*c. A look toward the future*

If we analyze the present situation with a critical eye, there are still reasons for research and development in the field of wave forecasting. Given the small errors quoted above, our hindcasts and forecasts never manage to get closer to the measured data no matter which model is used. Furthermore, different models, all using state-of-the-art physics and even the same input wind fields, generally lead to (albeit only slightly) different results. This is particularly the case when comparing the wave outputs involving different wind fields. Comparison of the results produced by seven major centers for the devastating Klaus storm in France and Spain, in the Western Mediterranean Sea, on 23-24 January 2009 (Bertotti et al. 2012) showed significant wave height differences of up to 20%. Indeed, although very sophisticated, there are still approximations embedded in our wave models. While the relevant processes are physically described, often the closure of small-scale processes is done empirically, by fitting measured data. Fitting, which is generally done on the bulk of the data, implies that the models are less accurate for the extreme—and hence rare, but frequently most important—events.

One reason for concern in the long term is the use of the spectral approach, which forms the backbone of the large majority of operational wave forecasting models. Notwithstanding the present excellent results, there is a growing belief that processes such as generation by wind and dissipation by white-capping (think of a severe storm) cannot be reduced to the sum of corresponding processes on a series of independently progressing sinusoidal waves. We do not have an alternative solution at hand, hence we continue with the idea of a spectrum as outlined by Pierson and Marks in 1952. Recent results (Cavaleri et al. 2015) derived from numerical simulations and direct observations suggest that the two basic processes, generation by wind and white-capping, are strongly related (Waseda et al. 2001) and should be treated as a single process, possibly also involving nonlinear interactions. A more complete reference and description of the present approaches in wind wave modeling and connected problems are given by Babanin et al. (2017, this volume).

## 4. Tidal and storm surge predictions

### a. *Early appreciation and development of tidal concepts*

Tides cause regular, large variations in the sea level on many coasts. Tides form the strongest currents in many shallow-shelf seas, and hence are crucial to navigation and port access. Tides are also important because of their interactions with tsunamis, storm surges and wind waves, and they are a primary source of internal waves, turbulence and mixing. Tidal dissipation slows the earth’s rotation. This section concerns the history of developing tidal concepts and prediction. Egbert and Ray (2017, this volume) give a summarized history but emphasize the state of the art of tidal prediction.

Storm surges (Fig. 6) are irregular, but can sometimes add several meters to the local tidal sea surface elevation, heightening to the flood risk. They also tend to correlate with damaging waves carried to shore on the excess level. Serious cases include the loss of 1795 lives in the Netherlands and 307 lives in eastern England on 31 January–1 February 1953; the loss of about 250,000 lives in Bangladesh (then East Pakistan) in November 1970 (Flather 2001); and the surge of up to 7 m from the Chittagong cyclone of April 1991, which killed 140,000 people in Bangladesh (Dube et al. 2009). Thus, there is a great need to predict tides and surges. The 1953 event in particular stimulated efforts to predict North Sea storm surges, although the interest extends to many areas around the world (WMO 2011).

Early evidence of tidal knowledge includes an Indian tidal dock from around 2000 BCE, and the writings of Aristotle (384-322 BCE) and Eratosthenes (275-195 BCE) on oscillating currents in the Euripus Channel (Tsimplis 1997). Tides were related to phases of the moon at Cadiz and in the Arabian seas, drawing on Arabian knowledge, while Chinese writers related the tidal bore near Hangzhou to phases of the moon. The Venerable Bede wrote (703 AD) of high waters progressing southtoward in the North Sea off the UK. Gerald of Wales

Figure 6. High tide plus storm surge over South Parade, West Kirby, Wirral UK, 5 December 2013.

similarly noted (1187) the different timings of floods and ebbs around the Irish Sea; he also remarked on the greater tides of the extensive Atlantic those of the Mediterranean. Such knowledge formed the basis for elementary tidal predictions. Tide tables using the lunar cycle existed before 1056 AD for the bore near Hangzhou, and from the early 13th century for London Bridge. There was also some appreciation that winds could affect water levels. However, all knowledge up to the 16th century was essentially empirical and not based on dynamical understanding.

Various attempts at a more dynamical explanation of tides in the 16th and 17th centuries preceded, and to some extent led to, Newton's Principia (1687), in which he proposed the inverse square law of gravity. For example, lunar gravity offset by the earth's acceleration toward the common center of mass causes a tide-generating gravitational potential, $\phi$,

$$\phi = -\frac{1}{2} G\, m_1\, r_e^2\, R_1^{-3} (3\, cos 2\lambda - 1) + O\left[ r_e^3\, R_1^{-4} \right] \qquad (2)$$

at a point $P$ on the earth's surface, where $G$ is the gravitational constant, $m_1$ is the lunar mass, $r_e$ is the earth's radius, $R_1$ is the distance between the earth and moon centers of mass and $\lambda$ is the angle between the directions from the center of the earth to point $P$ and to the moon. Any distinction between the common center of mass and the center of the earth will be small and included in the higher-order terms in (2). This potential led Maclaurin, Euler, and especially Bernoulli in the 18th century to develop the concept of the equilibrium tide $\zeta_e$, i.e., the surface elevation of the sea at rest: an equi-potential. The features to note are a raised elevation toward and away from the moon or sun, hence semi-diurnal tides as the earth rotates; larger fortnightly *spring* tides when the sun, earth and moon are in line, so that lunar and solar gravitational forces work together; and smaller *neap* tides when the moon is a quarter of the way around its orbit from the previous *spring* tide, so that lunar and solar gravitational forces partially cancel each other out. Diurnal tides depend on the sun or moon being overhead away from the equator, and hence they become much smaller at times near the equinoxes when both the sun and moon are almost over the equator. Smaller variations are associated with the ellipticity of orbits and the inclination of the lunar orbit to that of the earth around the sun. All of these features follow from Newton's formulation of gravity.

Harmonic analysis, for sinusoidal constituents of the tide at any particular location, was introduced by Laplace (1777, 1825), Thomson (1880) and Darwin (1883). All constituent frequencies are combinations of just six basic frequencies determined by astronomy and the earth's rotation via the evolving angle $\lambda$ in (2). Constituent amplitudes and phases need to be determined as a best fit to measurements. Computer models can now provide useful results, but the best estimates still use measurements, perhaps assimilated into a model. The Royal Society initiated systematic measurements in the 17th century, and time series covering periods from a fortnight to years became practical with the development of automatic recorders from the 1830s. Methods continue to evolve in the 21st century, including bottom pressure recorders and altimetry for mid-ocean tides.

Tidal predictions are enabled by re-combining constituents—an approach that gained practical application in the 1870s. A machine to perform the re-combination was invented by Thomson and constructed by A. Légé Engineering Company of London in 1872–1873 (Fig. 7). Lubbock (1830) introduced a non-harmonic *synthetic analysis and prediction* method relating the tidal amplitude and phase to astronomical variables. This method was the basis of the Admiralty Tide Tables for British ports from 1833 until about 1920. Doodson (1921) refined the harmonic method by introducing nonlinear constituents and using a better lunar theory. He also devised efficient schemes for harmonic analysis of data by hand computation. Harmonic analysis and re-combining of constituents remains the basis of modern predictions, although they are now performed numerically.

An alternative *response* method, introduced by Munk and Cartwright (1966), avoids the proliferation of constituents entailed by increasing the accuracy of the harmonic method. For an input equilibrium tide or nearby long-term record, the output surface elevation *response*, i.e., the output-to-input ratio, is assumed to be a slowly varying function of the forcing frequency. Measurements for the location of interest are used to estimate this response function (e.g., by fitting a low-order polynomial in frequency); a nearby long-term record may enable a lower-order fit. This approach also allows the identification of a component due to solar radiation.

Laplace (1777) developed Laplace Tidal Equations (LTE), *viz.*

$$\frac{\partial \vec{u}}{\partial t} - f\hat{k} \times \vec{u} = -g\nabla(\zeta - \zeta_e) \tag{3}$$

$$\frac{\partial \zeta}{\partial t} + \nabla \cdot [H\vec{u}] = 0 \tag{4}$$

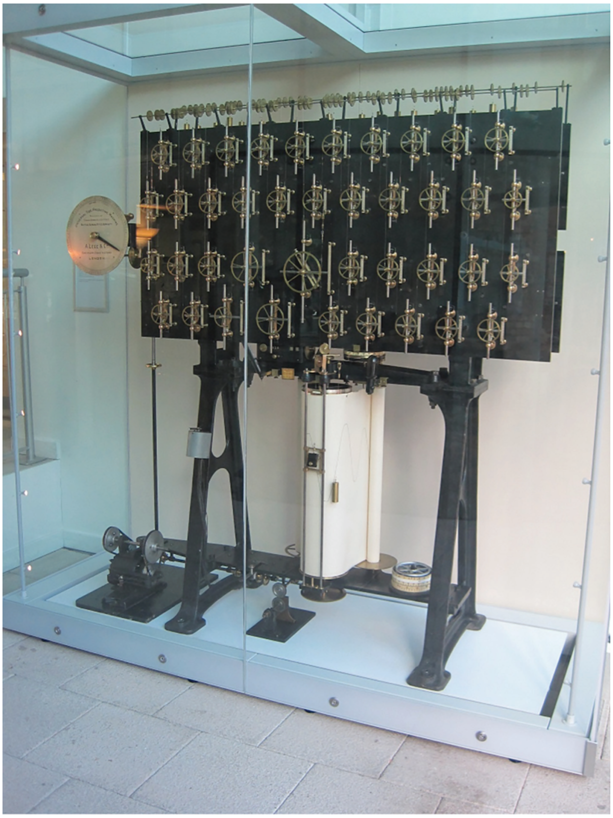

Figure 7. Roberts-Lg tide-prediction machine of 1906–1908 used for tidal predictions during World War II. At (UK) National Oceanography Centre, Liverpool, on loan from National Museums, Liverpool.

where $\vec{u}$ is the depth-averaged horizontal current vector, $t$ is time, $\hat{k}$ is unit vector in the vertical direction and $f = 2\Omega sin\theta$ is the Coriolis parameter with $\Omega$ the Earth's rotation rate and $\theta$ the latitude, $g$ is gravitational acceleration, $\zeta$ is the surface elevation, $H$ is the still water depth and forcing is by the equilibrium tide $\zeta_e$. The latter represents the tidal forcing frequencies and the forcing structure. The ocean response to this forcing shows large ranges in shallow shelf seas, cyclonic propagation around ocean basins (due to the Coriolis acceleration) and limitation of the propagation speed to $\sqrt{gH}$, where $H$ is the basin's depth, of the order 200 $ms^{-1}$. Ocean basins with a complex shape have their own natural periods of oscillation, which affect the form of the tidal response in space and time.

Young (1813) introduced bottom friction $\tau_b$ proportional to $|\vec{u}|^2$ in LTE and devised the mapping of co-tidal lines (lines of equal tidal phase) on a chart to represent the propagation of a constituent. Since the 1830s, Lubbock (1830, 1836), then Whewell (1833) and others have attempted to map cotidal lines. Whewell tried it for the world's oceans based on progressive waves, while Harris (1904) attempted to represent ocean tides as a combination of standing waves.

Progressive wave solutions are the *building blocks* of LTE. These wave solutions are composed of Kelvin waves that propagate along a coast with a decreasing amplitude offshore (Thomson 1880) and plane progressive Poincaré waves at frequencies greater than the Coriolis frequency (Poincare 1910). Proudman (1917) developed a theory of tides in ocean basins of any shape as a combination of basis *Proudman* functions (forms of natural oscillations). Flather and Davies (1976) defined the appropriate open lateral boundary conditions for tidally forced, limited-area shelf seas and basins. LTE can also represent the effects of nonlinearity, the elastic earth and changes of gravitation due to tidal deformation of the earth and ocean (Hendershott 1972; Farrell 1973). The best spatial representations of tides produced since the 1980s use numerical models representing LTE to assimilate *in situ* measurements and, since the 1990s, altimetry, see Stammer et al. (2014).

The response method of analysing observational records, and the distributions of amplitudes and phases from applying LTE, benefit predictions mainly via the interpolation between locations where observed long time series enable accurate harmonic analysis and recombination. LTE can model consistently tidal currents and elevations consistently, whereas the tidal current measurements are difficult and sparse in most areas.

### *b. Development of surge predictions*

Storm surges are caused by meteorological forcing: atmospheric pressure and especially winds that add to tides. The factors that may contribute to the severity of impact, depending on the context, are extensive shallow coastal waters, converging coastlines ("funnelling"), high tides, low-lying land, prevalent cyclone tracks, and river discharges (all factors summarized by Dube et al. (2009) with reference to Bangladesh). There can be enhanced responses: *Proudman resonance* if an atmospheric disturbance progresses near the long wave speed $\sqrt{gH}$ (Proudman 1929), and the equivalent *Greenspan resonance* for edge waves along a coast (Greenspan 1956) or if the forcing frequency and pattern match a natural form of shelf-sea oscillation. The term *meteotsunami* has been used where such an enhanced response, shoaling, refraction, and/or run-up lead to inundation several meters above the predicted level for tides alone (Pugh and Woodworth 2014).

Given the conceptual understanding of meteorological forcing, the first approach to sea level prediction attempted to correlate the surface elevation with the atmospheric pressure, wind speed and direction using long time series of these variables. "Tide gauges" for recording surface elevation date back to the 19th century in some North Sea locations, enabling the study of correlations (Flather 2001). The approach was developed from the 1920s by Doodson and co-workers, as outlined in Defant (1961), and was applied in particular to the 1953 North Sea surge (Rossiter 1954). Depending on the location, the square of the wind speed, $u_w^2$, may be a better predictor than simply wind speed as could winds from a remote forcing region be more important than the local ones (Amin 1982). An extension of this approach using artificial neural networks was proposed more recently (Sztobryn 2003).

Sea basins, atmospheric pressure and wind forcings are complex in space and time but are readily incorporated into the shallow water equations (SWE, generalizing LTE):

$$\frac{\partial \vec{u}}{\partial t} + \vec{u} \cdot \nabla \vec{u} - f\hat{k} \times \vec{u} = -g\nabla(\zeta - \zeta_e) + \nu \nabla^2 \vec{u} - \frac{1}{\rho}\nabla p_a + \frac{1}{\rho}\frac{(\vec{\tau}_a - \vec{\tau}_b)}{(H + \zeta)} \quad (5)$$

$$\frac{\partial \zeta}{\partial t} + \nabla \cdot [(H + \zeta)\vec{u}] = 0 \quad (6)$$

Notation here is as for equations 4; $\nu$ is the kinematic viscosity, $\rho$ is the sea density supposed to be constant, $\vec{\tau}_b$ is the bottom stress; forcing is by the equilibrium tide $\zeta_e$, the atmospheric wind stress $\vec{\tau}_a$ and the atmospheric pressure $p_a$.

Some simple steady-state balances (Flather 2001) are

1. $\zeta = -\frac{1}{g\rho} p_a$, the inverse barometer,
2. set-up by wind stress $\nabla\zeta = \frac{1}{\rho g H}\vec{\tau}_a$.

However, analog or numerical solutions are generally necessary. Analogs include laboratory models and electronic representations with capacitors, for example, developed in the 1960s and 1970s by Ishiguro (1972) before numerical models found favor. Currents consistent with surge elevations (as for tides) are modeled by the SWE, whereas their measurement is difficult and sparse. The sensitivity of surges to winds has led to continual development of the formulation of wind stress $\vec{\tau}_a$ from the 1960s to the present (Horsburgh and De Vries 2011).

Hansen (1956) proposed a numerical scheme to represent equations (5) and (6), and applied it with encouraging success to the 1953 North Sea surge. Numerical models for tides and storm surges were developed through the 1960s and 1970s: Jelesnianski (1965) and Reid and Bodine (1968) in the US, Robinson et al. (1973) for the Adriatic and Venice, Dronkers (1969) and Heaps (1969) for the northwest European continental shelf. For tides alone, an appropriate open boundary condition for limited-area shelf seas and basins is that arriving (inward) radiation is not affected, i.e., the locally-determined perturbation radiates purely outward (Flather 1976). This lateral boundary condition derives from a mass conservation constraint, as shown many years later by Oddo and Pinardi (2008).

The accuracy of storm surge predictions depends on the good representation of bathymetry (with sufficient model resolution), meteorological forcing and waves in combination with surface and bottom stress formulations, as shown by de Vries et al. (1995) through inter-model comparison. An adjoint model has been used to determine the sensitivity of the surge level at a coastal location to perturbations in wind stress, depending on location and time lag (Wilson et al. 2013). A further discussion of numerical formulations can be found in (Horsburgh and De Vries 2011).

Where the nearshore area slopes gently, predictions may be improved by a moving coastal boundary, representing inundation, as distinct from imposing a zero normal flow (Yeh and

Chou 1979). Flexible grids developed since the 1970s can improve the fit to coastlines, enable fine resolution of critical areas (see examples in Horsburgh and De Vries 2011); they have been used to simulate inundation with varying success (Chen et al. 2013). Three-dimensional models can better represent bottom stress in particular. Large tides and strong surges may interact in shallow water through nonlinear terms in the equations, as shown for the North Sea by Prandle and Wolf (1978). In particular, an enhanced tide plus surge elevation travels faster than the tide alone because the water is deeper. Therefore, the peak surge tends to arrive before the predicted time of high water. The concept of a "skew surge" (the difference between the predicted level at high tide alone and the nearest experienced high water level) is most relevant to the additional flood risk due to a surge. Lisitzin (1974) showed that Baltic Sea storm surge amplitudes are smaller when ice is present. Several studies have examined the influence of ice on surges in Canadian waters (reviewed by Murty et al. 1995). Ice influences the effective fetch, surface waves and transmission of stress from air to water; it also damps long waves (Horsburgh and De Vries 2011). Coupling of waves for their momentum input and to improve the representation of stresses has been considered since the 1990s, e.g., Brown et al. (2013).

Forecast systems have been operational since the late 1970s in Belgium (Adam 1979) and the UK (Flather 1979). Usual practice is to form a best estimate of the total level as

$$\begin{aligned}\textit{best}\text{ estimate of sea level} = {} & (\text{modeled tide}+\text{surge}) - (\text{modeled tide}) \\ & + (\textit{best}\text{ prediction of tide} + \text{other contributions not modeled})\end{aligned}$$

This allows for a nonlinear interaction between tide and surge, and for the possibility that the model does not produce the best prediction of tides or of all contributions to the total level; waves may be added to the surge here if jointly modeled. However, this practice uses only the operational model tide (not necessarily the best) for the interaction. Zijl et al. (2013) discuss the maximal use of data and adjustment of the model parameters to improve operational tide modeling sufficiently to obviate a separate tidal prediction.

Observational networks that provide elevation data in (near) real time are essential to support predictions (Flather 2000). The data may be assimilated into the models to improve the initial conditions for forecasts. The Dutch operational system has applied data assimilation since 1992, using antecedent elevations from the UK east coast (Flather 2000), thereby improving forecasts on the Dutch coast during the first 10 hours or more. Observational data are invariably used to validate and check the model predictions using developments in model assessment methods (Lynch and Davies 1995).

Storm surge model forecasts using an ensemble of weather forecasts (varied to represent uncertainties in atmospheric pressure and wind forecasts) were tested successfully in the 2000s to estimate prediction uncertainty. They became operational at, for example, the UK Met Office in December 2009 (Flowerdew et al. 2010) with an extension to 7.25-day forecasts in summer 2011 (Flowerdew et al. 2013). Slightly varied initial conditions and model parameterizations are also appropriate to form an ensemble (Horsburgh and De Vries 2011).

Predictions of statistics of extreme levels (mean sea level plus tide plus surge plus waves) and strong currents are needed to assess flood risks and to design coastal and offshore structures. Methods of combining tide and surge statistics were developed from the 1970s with subsequent consideration of spatial and temporal extent of events (e.g., Dixon and Tawn 1992). Time series of many years or even decades are used with statistical distributions specific to extremes. Model runs "calibrated" by measurements can be valuable if the measurement time-series are not long enough (e.g., Davies and Flather 1987; Flather 1987).

Extreme levels are expected to continue to rise because of rising mean sea levels due to global warming. The chance that surges and tidal ranges may increase and cause to additional extreme events almost certainly depends on location and is the subject of continuing research (Weisse et al. 2014; Arns et al. 2015).

## 5. Ocean mesoscale predictions: the Harvard School

### *a. Mesoscale discovery and hindcasting*

As already illustrated for weather, waves and storm surges, all forecasting methodologies originate from the analysis of specific observations to ensure the quality of the initial conditions for the forecast and from the choice of an adequate predictive model for the phenomena of interest. This methodology has also been the basis of scientific developments in open-ocean, 3D current forecasting.

Three-dimensional ocean currents, temperature and salinity fields are dominated by the "ocean weather" or mesoscale (see Treguier et al. 2017, this volume). Robinson (1983) describes mesoscale variability as follows: "Ocean currents and their associated fields of pressure, temperature, and density vary energetically in both time and space throughout the ocean. Such variability in fact contains more energy than any other form of motion in the sea. Partly organized, yet highly irregular, these motions have dominant spatial scales in the range of tens to hundreds of kilometers and dominant temporal scales in the range of weeks to months." If ocean current forecasting were to be attempted, the mesoscale would need to be mapped because it comprises so much of the initial state of any ocean forecast. The mesoscale initialization problem was the crucial issue to overcome before ocean forecasting could become a reality.

Mesoscale temperature, salinity and velocity fields were mapped for the first time in the 1970s, first by the Russian POLYGON experiment (Koshlyakov and Grachev 1973) and then by two large international MODE ("MODE Group" et al. 1978) and POLYMODE (Osborne and Rizzoli 1982a) programmes in a $500 \times 500\ \text{km}^2$ area in the subtropical gyre of the North Atlantic (Fig. 8; Robinson and Haidvogel 1980). Objective analysis techniques based on the meteorological experience (Gandin 1965) and customized for oceanic flow fields (Bretherton et al. 1976) were developed and applied to these large observational arrays (McWilliams 1976; Carter and Robinson 1987) to generate the maps and initial conditions for mesoscale hindcasts.

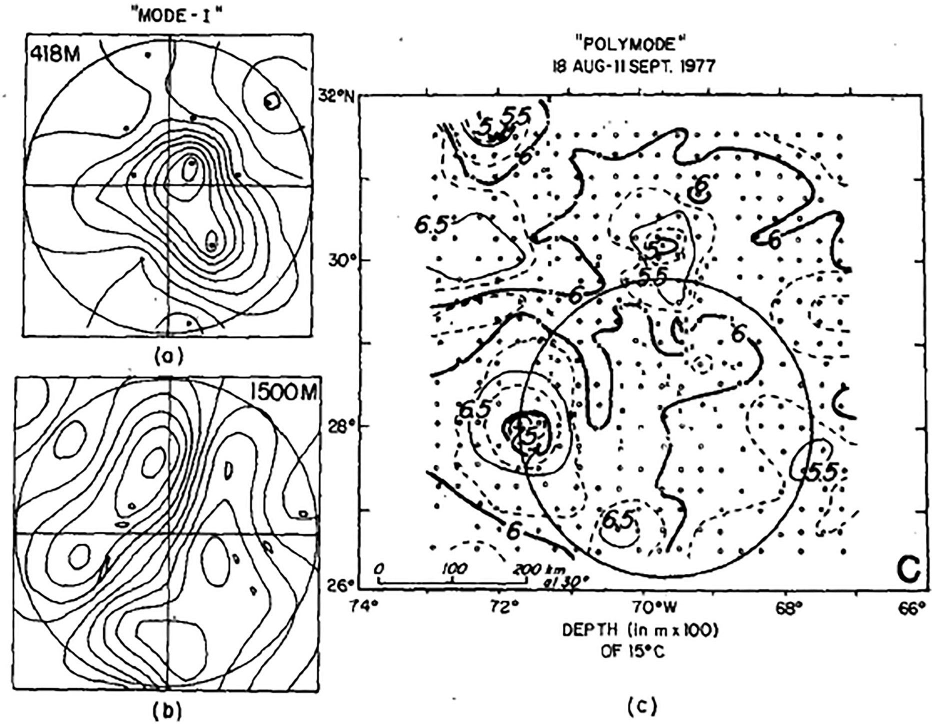


Figure 8. Mesoscale synoptic maps (a) at 418 m for the temperature field (contour interval 0.1 C) and (b) at 1500 m for the streamfunction field for the MODE-I region and (c) from the POLYMODE larger area for the depth of the 15 C isotherm (units meters × 100). The circle is the same in the three pictures (reproduced from Robinson and Haidvogel 1980).

The first dynamical ocean forecast paper to discuss the limits of predictability in mesoscale ocean regimes was Robinson and Haidvogel (1980). These authors discuss several twin-like experiments that were dedicated to understanding the growth and propagation of errors in a limited-area, barotropic, quasigeotrophic model due to the updating frequency of the lateral boundary conditions, the initial condition and the accuracy of the numerical scheme. Their results indicated that forecast quality depends more on the updating frequency of the stream function at the lateral boundaries than on the accuracy of the specified vorticity field. The predictability time was longer than the few days in the atmosphere (Lorenz 1982) due to the instability growth time scales of the ocean being longer than those of the atmosphere. The study showed that the same kind of quasigeostrophic numerical model as used for the first atmospheric forecast (Charney et al. 1950) could reproduce realistic features of the oceanic mesoscale field.

An open-ocean, baroclinic quasigeostrophic model was then developed at Harvard (Miller et al. 1983; see Appendix A) and used to conduct extensive hindcast experiments. The

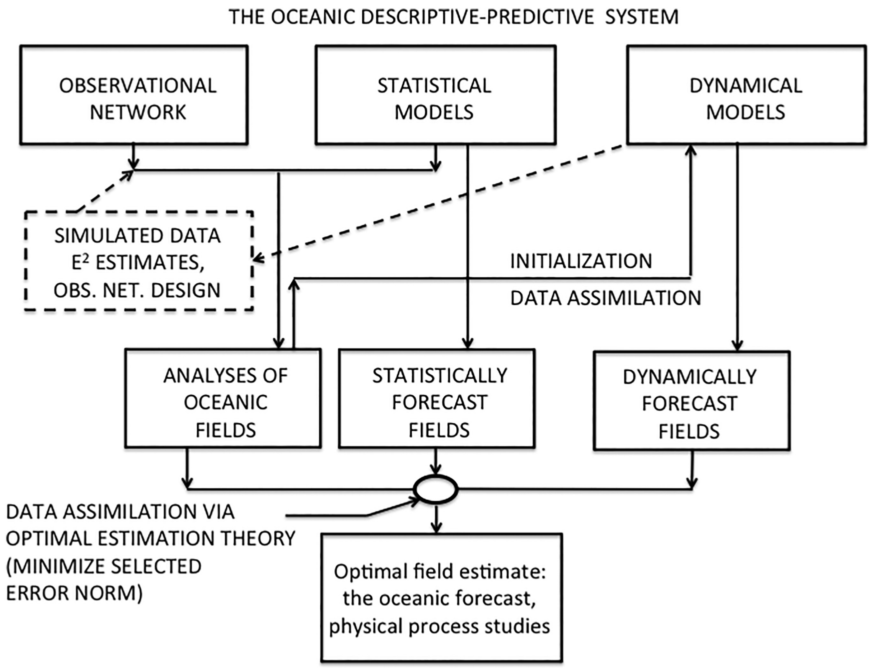


Figure 9. The general scheme of the descriptive predictive system developed at Harvard at the beginning of the eighties (reproduced from Robinson and Leslie 1985).

model was initialized using the dynamic height computed from POLYMODE temperature and salinity data (Carton 1987; Pinardi and Robinson 1987; Robinson and Walstad 1987). The predictability time was again long, of the order of several weeks up to a month, because it referred to deep mesoscale structures, from 700 to 1400 meter depth in the water column. These important hindcast experiments showed that an "oceanic descriptive-predictive system" could be designed that would offer forecasts in a highly nonlinear mesoscale field such as the open ocean subtropical gyre region. The first scheme of an oceanic predictive system, reproduced in Figure 9 from Robinson and Leslie (1985), illustrates the methodology of ocean forecasting, encompassing the observations and statistical techniques required to produce realistic initial conditions.

*b. The 1983 first real-time forecast in the California region*

In summer of 1983, a collaboration between A. R. Robinson of Harvard University and C. N. K. Mooers of the Naval Postgraduate School of Monterey, CA (Robinson et al. 1984, 1986) carried out the first real-time forecast in the mesoscale eddy field of the California Current system using the Harvard descriptive-predictive system described in Figure 9.

The experiment involved collecting synoptic profiles of temperature and salinity and transforming them into geostrophic streamfunction fields from the surface to the bottom of

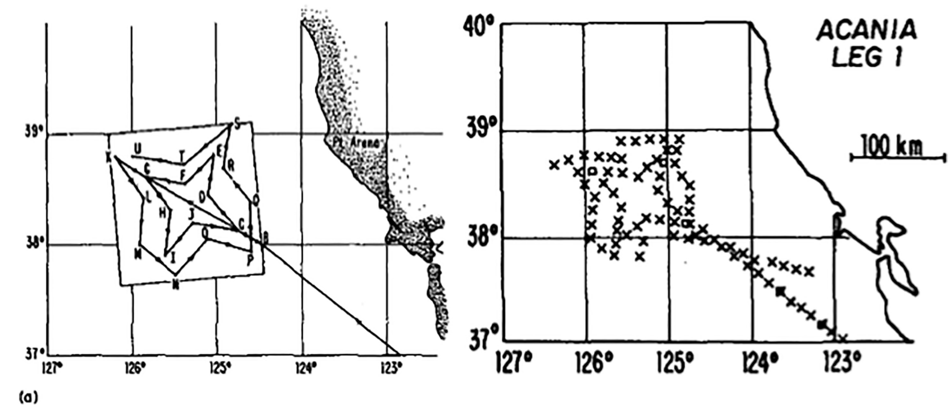


Figure 10. The first real-time forecast experiment carried out in the California Current mesoscale eddy field. Left panel: the cruise track design within a 150 × 150 square. (B-U) indicate the ship route in time. Right panel: actual data collected along the path, crosses indicate 450 m deep XBTs and empty squares indicate 1000 m deep CTD profiles. (reproduced from Robinson et al. (1986)).

the ocean. Measurements were carried out with a specific sampling network (Fig. 10) that allowed the use of a few 1000-m Conductivity Temperature Depth (CTD) casts interspersed with 450-m XBT (eXpandible BathyThermograph) to collect 10-km resolution profiles in a 150 × 150 km$^2$ rectangle within the synoptic time scale of one week. This innovative observational methodology was developed to be able to derive proper vorticity fields for the Harvard baroclinic quasigeostrophic model. The zig-zag cruise track allowed control of the second derivatives of the streamfunction field, i.e., the relative and thermal vorticity (see Appendix A). In addition to this novel sampling methodology, an innovative methodology had to be developed to "extend" the information from the 450-m depth of the shallower profiles to the bottom of the region, at about 4200 m. The first extension procedure made use of baroclinic and barotropic vertical modes computed from historical CTD data. The extension was later improved with the use of empirical orthogonal functions (Robinson et al. 1986; De Mey and Robinson 1987). Three cruises, spaced about two weeks, were carried out in order to have initialization and forecast validation data sets. The Harvard quasigeostrophic model was implemented with six levels and a horizontal resolution of about 9 km, which would be defined as eddy permitting because the local Rossby radius of deformation is about 25 km. The baroclinic initial and verification streamfunction fields for June 20, 1983 and July 4, 1983 are shown in Figure 11. Within two weeks the flow field evolved rapidly: two baroclinic anticyclonic eddies are present at initial time (the experimental domain captured only the borders) while, two weeks later, only one is evident with a long tail and large velocities in the center of the domain. This evolution was understood to be a violent eddy merger event occurring in two weeks and never experimentally observed before in the ocean (Robinson et al. 1986).

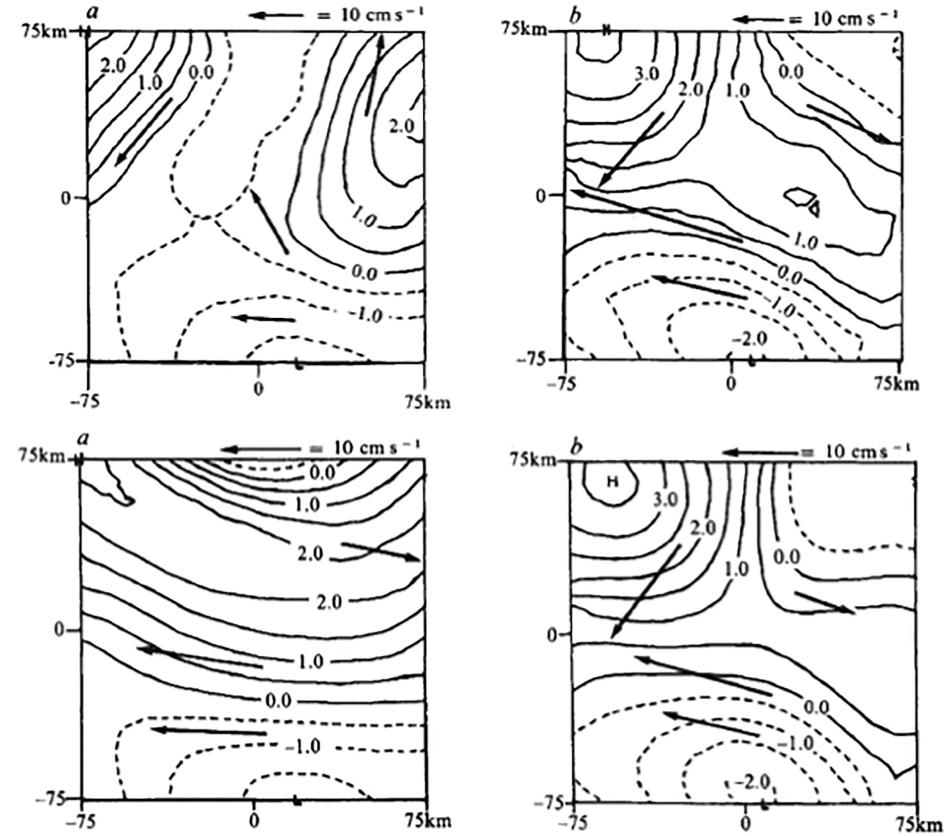


Figure 11. The first real time forecast experiment carried out in the California Current mesoscale eddy field. Top left image: the initial streamfunction field at 150 m depth for June 20, 1983 calculated from observations. Top right image: the streamfunction field after two weeks (July 4, 1983) as deduced from observations. Bottom left image: the real time forecast for July 4, 1983. Bottom right image: the re-forecast streamfunction field for July 4, 1983. In all images, arrows indicate current speed direction, the scale of the streamfunction is 5000 $m^2s^{-1}$. (Reproduced from Robinson et al. (1984)).

The results of the first forecast are shown for the upper 150-m stream function field in Figure 11. The real-time, two-week long forecast was done with persistence lateral boundary conditions and was capable of correctly simulating the dynamical development of the merger event between the two anticyclonic eddies. After the second data collection exercise, lateral boundary conditions could be linearly interpolated between June 20 and July 4, 1983, thus giving rise to a re-forecast experiment that was extremely successful in simulating the large nonlinear evolution of the flow field (Fig. 11). The success of the forecast is evaluated in terms of the demonstrated capability of the numerical model to properly capture the dynamical evolution of the flow field, i.e., the eddy merger process, even with persistence lateral boundary conditions. We argue that the quality of the first ocean forecast is greater than the one of the atmospheric forecast conducted 30 years earlier, even if in both cases a simple quasigeostrophic model was used. The greater accuracy of the ocean forecast was probably due to the use of a baroclinic instead of a barotropic model (see Appendix A) and the greater accuracy of the initial conditions for a limited region of the world's oceans. The flow field in Figure 11 is characteristic of the upper thermocline layer and it is appropriately described by quasigeostrophic dynamics. The quasigeostrophic model used for the first forecast did not consider Ekman pumping or density changes caused by air-sea interactions because, during the summer period, the flow field might have been independent from direct driving from the atmosphere. Again, the predictability time scale is long, about two-weeks, due to the dominant geostrophic regime.

The California current forecast not only demonstrated that there is predictability over a two-week time scale, even in a highly nonlinear ocean eddy field, but showed also the importance of forecasting for the study of fundamental ocean processes. The eddy merger process captured by the observations and the model forecast made it possible, for the first time, to study the mixed barotropic-baroclinic instability processes that act in an oceanic realistic flow field, using the dynamical and energy balances built into the numerical model (Pinardi and Robinson 1986; Robinson et al. 1986).

### *c. The 1984 Gulf Stream forecast*

Following the success of the California Current experiment, the Harvard oceanography group moved to explore the potential predictability of the oceanic 3D flow field in a much more difficult regime to forecast: the Gulf Stream system with its meanders and ring-formation areas.

This time, the initialization procedure had to use synoptic satellite information and "extension" procedures based on a "Feature-Model" initialization method, a much more sophisticated procedure based on the dynamical knowledge of the Gulf Stream and ring structures obtained from climatological studies. This initialization procedure was the first to be used for forecasting, and it encompasses all of the concepts of modern data assimilation for surface satellite observations. In other words, at this early stage the "Feature-Models" substitute the background error covariance when inferring the subsurface dynamical fields from the surface observations. To clarify this concept, let us take the example of a cyclonic ring observed in Sea Surface Temperature (SST) satellite images. The low SST values in the ring core correspond to uplift of the temperature isotherms near the vortex center. In turn, the cyclonic eddy has a subsurface velocity structure that has been recorded in other process-oriented studies. Knowing the analytical relationships between SST and subsurface ring temperature and velocity structures allows one to create the ring initial condition geostrophic streamfunction fields throughout the water column, as illustrated in Figure 12. Robinson et al. (1988) called this a "Feature Model" initialization/extension procedure that nowadays is carried out by sophisticated data assimilation schemes.

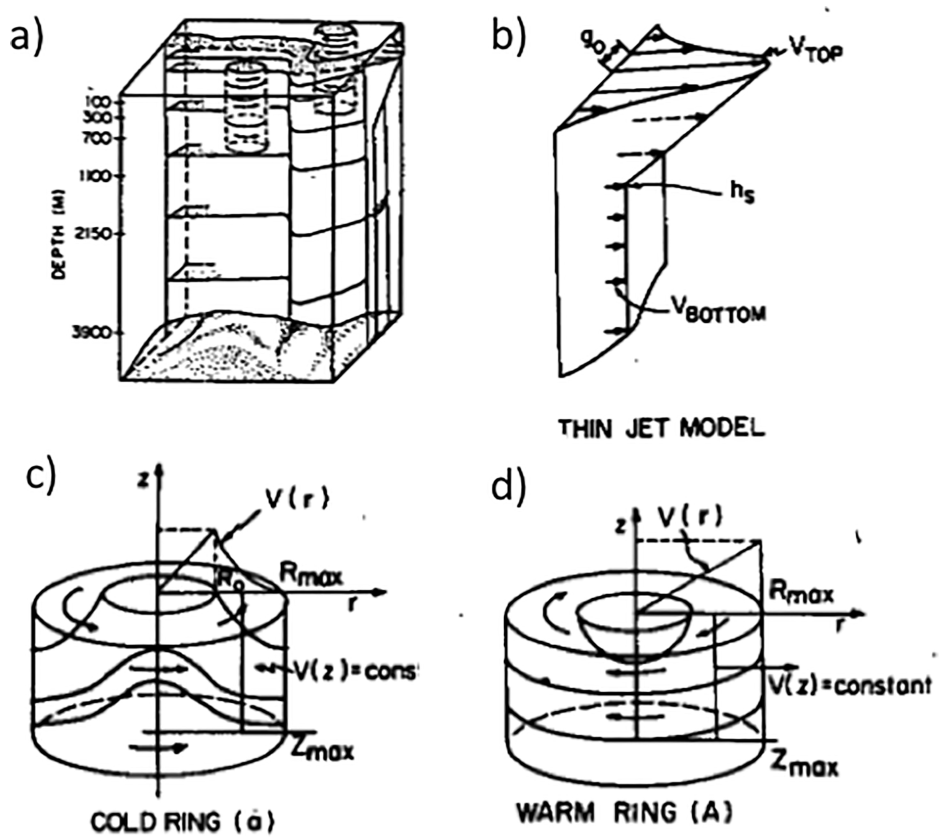


Figure 12. The "Feature Model" initialization procedure for the Gulf Stream forecast system. a) The vertical and horizontal positions of the Gulf Stream current profile with warm and cold core rings on its warm and cold sides respectively. This image is made using only satellite SST observations of the temperature fronts to locate the Gulf Stream and the ring positions. b) The along-stream current velocity profile as a function of the cross-stream coordinate and depth. c) Cold ring and d) warm ring velocity profiles with different parameters that were identified from climatological studies. (Reproduced from Robinson et al. 1988).

The first Gulf Stream forecast was carried out with the baroclinic quasigeostrophic model described earlier, as in the California current case and using the "Feature Model" initialization (Robinson et al. 1988). In Figure 13, we show the initialization and the 19-day forecast stream function where two intense and, in principle, very nonlinear processes occurred. The first is the cut-off of a cold core ring that was detached at day 15, probably 3–4 days earlier in the model than in the observations. The second is the absorption of a warm core ring in the stream, which produced a contorted meandering of the stream with great similarities to the satellite frontal position observations.

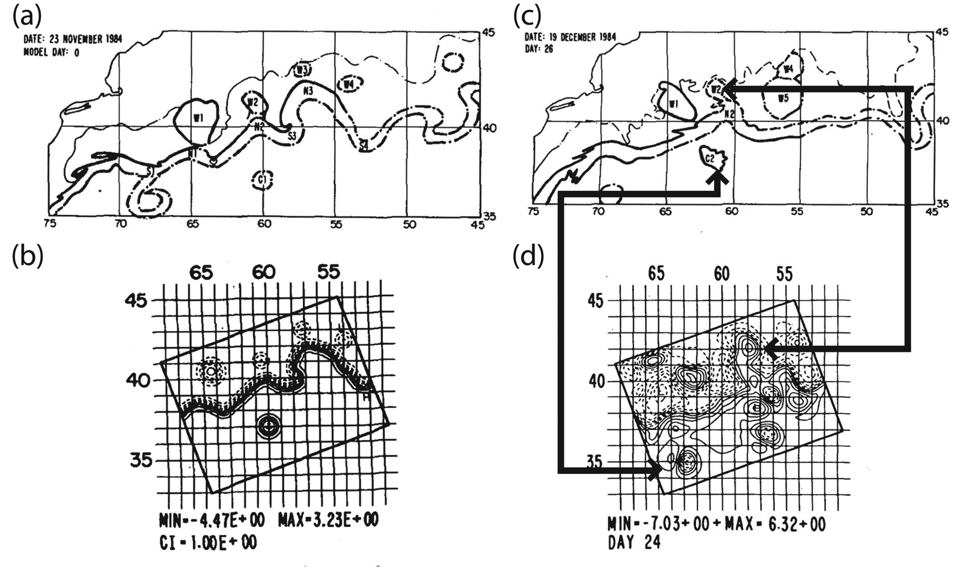


Figure 13. In the top left panel, the satellite SST frontal position analysis from NOAA for November 25, 1984, used to produce the quasigeostrophic streamfunction initial condition at 300 m for the Gulf Stream area, shown in the bottom left panel. In the top right panel, the satellite SST frontal position analysis for 14 December 1984 is compared with the 19 day forecast streamfunction field at 300 m (reproduced from Robinson et al. 1988).

Again, ocean forecasting was demonstrated to be feasible over time scales of a few weeks for the deep thermocline flow field. At this time, uncertainties connected to atmospheric forcing were not considered, the forecast was "feature oriented" and the specific model chosen filtered out processes that were much more unpredictable, such as surface and mixed-layer temperatures, salinity and velocity fields, shorter time-scale processes such as inertia-gravity waves and barotropic sea level variations across the Gulf Stream.

While the Gulf Stream forecasting with the quasigeostrophic model was consolidated to deliver operational forecasts for the U. S. Navy, a new primitive equation forecasting model was developed and adapted to forecast in the Gulf Stream region (Robinson et al. 1989; Spall and Robinson 1989), increasing the accuracy of the forecast and starting to address the mixed layer predictability issues.

*d. The key issue: assimilation of satellite altimetry*

The advent of the U. S. Navy GEOSAT (McConathy and Kilgus 1987) at the beginning of the 1980s and its declassified geophysical data records at the beginning of the 1990s made it clear that mesoscale ocean mapping was feasible with altimetry. Even before the GEOSAT data were available, the Harvard group carried out fundamental studies of ocean hindcasting with initialization from ocean-altimetry-like observations (De Mey and Robinson 1987) using the POLYMODE temperature and salinity profiles.

The major issue for the initialization and assimilation of satellite altimetry is the vertical "extrapolation/extension" method for sea surface height observations. It was recognized early on that the observed sea surface height from altimetry was not capable on its own of constraining the subsurface fields even in a quasigeostrophic model (Berry and Marshall 1989): only two-level quasigeostrophic models or two-layer primitive equation models (Hurlburt 1986) could dynamically transfer the information from the surface to the subsurface because of the direct relationship between surface pressure and interfacial layer displacements and/or interface vertical velocities (Cushman-Roisin and Beckers 2011). In the case of multi-level or multi-layer models, statistical "extrapolation/interpolation" techniques should be used.

The Harvard group was the first to use such statistical techniques to "extend/extrapolate" the sea surface height into subsurface fields for forecast/hindcast initialization. They simplified the problem using the Harvard multi-level quasigeotrophic model, in which all of the dynamical prognostic variables, pseudopotential vorticity and density can be inferred from a 3D stream function. To order Rossby number (Appendix A), the surface streamfunction field is equivalent to the sea surface height, as it could be measured by an altimetric satellite. Furthermore, they used the POLYMODE observations (Osborne and Rizzoli 1982b), transformed into a 3D streamfunction field derived from the dynamic height field, to statistically analyze the stream function vertical variance via Empirical Orthogonal Functions (EOF; Navarra and Simoncini 2010). The data assimilation scheme is reproduced in Figure 14 from De Mey and Robinson (1987). In this picture, the scheme is depicted as being comprised of the objective analysis scheme, used to horizontally map the POLYMODE observations, and the vertical "projection/extension" procedure done using the vertical EOFs computed from the POLYMODE dynamic height fields. Vertical EOFs are still used today in 3Dvar assimilation schemes to model the background error covariance matrix vertical structure, and to extend the assimilated sea surface height anomalies to subsurface dynamical state variables (Dobricic and Pinardi 2008; Storto et al. 2011).

The results of assimilating the sea level anomalies derived from the POLYMODE observations, sampled along different satellite altimetry tracks (with repeat cycles from 10 to 22 days) across a $250 \times 250\ \mathrm{km}^2$ domain, are shown in Figure 15. The Harvard quasigeostrophic model is initialized following the procedure described in Figure 14, in particular, using the surface streamfunction reconstructed from satellite track information and extrapolating the streamfunction in the deep levels using one vertical EOF computed from POLYMODE *in situ* data (De Mey and Robinson 1987). The results show two remarkable facts: 1) the initial errors at 100 m double after 15–30 days, thus confirming the relatively long predictability time of ocean fields; 2) the deep model levels (1400 m) extrapolation method with EOFs enables a 70%–80% reduction of the root mean square error (RMSE) in about 30 days. This error reduction would not have happened without the extrapolation of the surface streamfunction (as shown in De Mey and Robinson 1987), suggesting that the model is capable

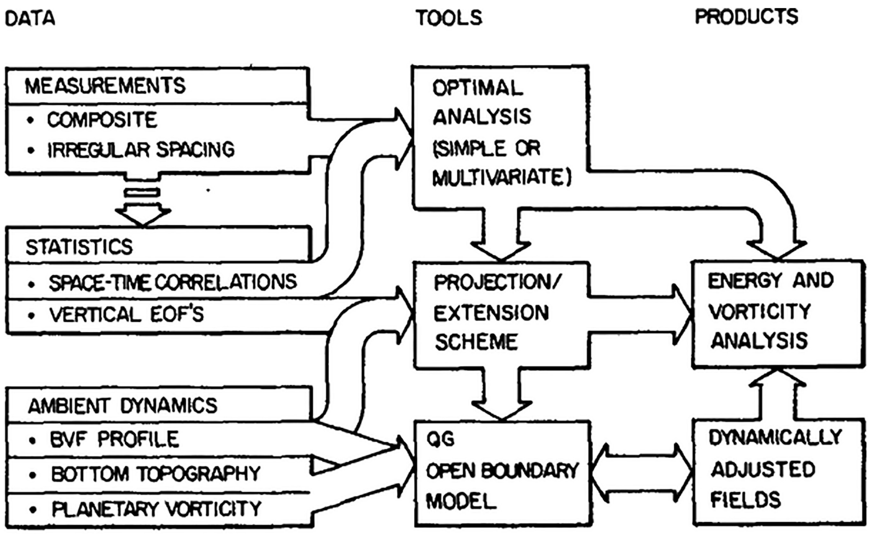


Figure 14. The data assimilation scheme for initialization of hindcasts in the POLYMODE North Atlantic subtropical gyre area using "extrapolation" of altimetric-like observations to the deep ocean. The diagram is subdivided vertically in three components: the first is the "Data" component that contains all the observations and the methods useful to initialize the forecast/hindcast: "composite" means different types of measurements with irregular spacing, both from satellite and *in situ* sensors, "statistics" means knowledge from historical measurements of space-time correlations and vertical Empirical Orthogonal Function structures, "ambient dynamics" contains Brunt-Vaisala frequency (BVF) profiles from climatological data, used in the quasigeostrophic model (see Appendix A). The second component is called "Tools" and contains the diagnostic algorithms and the prognostic model: optimal analysis here means objective analysis to produce an initial condition in the model numerical grid, the specific vertical projection/extension scheme to be used for satellite altimetric data sets and the quasigeostrophic model (QG) with lateral open boundary conditions. The third component are the "Products" that consist of analysis of energy and vorticity balances to understand the local dynamics and the hindcast fields, so-called in the diagram "dynamically adjusted fields" (reproduced from De Mey and Robinson (1987)).

from a statistical initial guess to cascade energy to the barotropic mode, that is, the dominant energy-containing mode at these depths and in this region.

In the late 1980s, the U. S. Navy began developing synthetic vertical temperature and salinity profiles derived from the observed sea surface heights and temperatures, based on the work by Dewitt (1987) and Carnes et al. (1990). The ultimate goal of this work was to use the real-time satellite altimeter missions to enable nowcasts of the global 3-D temperature and salinity fields, and to initialize the primitive equation ocean forecast models developed by the U. S. Navy that would allow the prediction of ocean mesoscale eddies.

These satellite altimetry studies were the basis for the development of operational oceanography in the years to follow. They demonstrated the need for statistical vertical

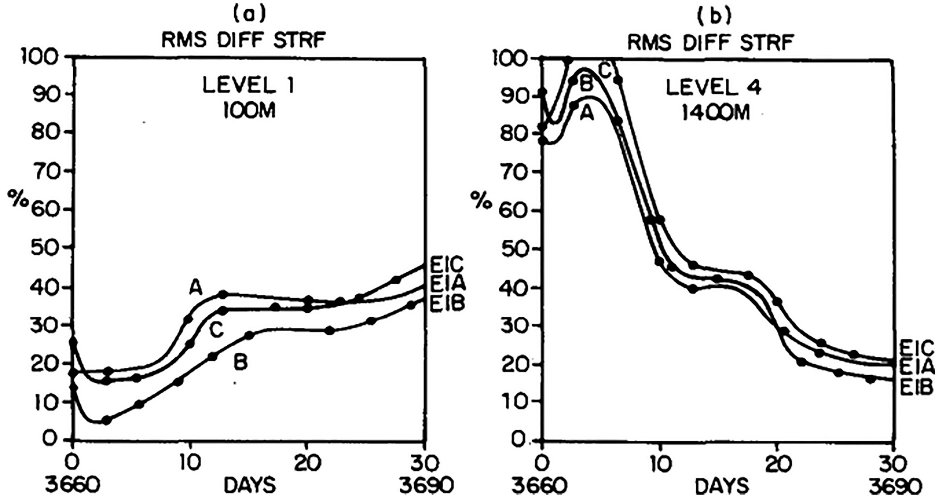


Figure 15. The Root Mean Square Error (RMSE) evolution for a 30 days hindcast in the POLYMODE region (reproduced from De Mey and Robinson 1987) assimilating three different satellite-like altimetric data with three different repeat orbits (10, 22 and 17 days, A, B, C, respectively, in the panels). Left panel: RMSE as a percentage over the field standard deviation at 100 m. Right panel: RMSE as a percentage over the field standard deviation at 1400 m.

extrapolation methods to assimilate the sea surface height from altimetry. The study by Mellor and Ezer (1991) was one of the first to use the assimilation of satellite altimetry to initialize a primitive equation model, where the sea surface height observations were correlated with the subsurface salinity and temperature profiles with a simple statistical regression relationship. Finally, the problem of vertical "extrapolation" of the altimetric sea surface height was simplified and dynamically justified by Cooper and Haines (1996). De Mey and Robinson (1987) and Cooper and Haines (1996) set the path for sea surface height altimetry data assimilation in modern operational forecasting systems.

## 6. Regional and relocatable ocean forecasting systems

After mesoscale predictions were shown to be successful, regional prediction systems that focused on specific areas and oceanic regimes of interest were developed. In a sense, weather predictions also started early with regional models (Hill 1968; Wang and Halpern 1970; Miyakoda and Rosati 1977) and showed the importance of high-resolution regional modeling in increasing the forecast skill. The Gulf Stream forecasting system illustrated in the previous section was the first example of a regional ocean forecast system, and it was useful for the U. S. Navy open sea operations.

The concept of a regional forecasting system was again developed by A. R. Robinson (Robinson 1992; Robinson et al. 1996) and was transformed at the end of the 20th century into a *relocatable* forecasting system for rapid assessment of the coastal environment (Robinson and Sellschopp 2002). The concept is that if either broad-scale sampling surveys of ocean conditions, or coarser-scale, larger-domain models, can provide the initial and lateral boundary conditions with sufficient accuracy, then a semiautomatic set of protocols can be applied to downscale and nest higher-resolution ocean models that will better resolve the dynamics and the local processes. Robinson et al. (1996) describes how to build the regional systems as follows:

> [The consideration for, *author entry*] a regional real-time forecasting system proceeds in three phases, based on previous knowledge and experience of the area. In the initial (exploratory) phase, identification of dominant scales (synoptic, mesoscale and submesoscale), processes, and interactions is obtained. In the intermediate (dynamical) phase, a clear resolution of the important dynamics and events must be reflected in the nowcasts and forecasts. This is carried out via energy and vorticity analysis. The third phase is designed to validate the predictive capability of the forecasts. Both qualitative verification and quantitative skill are utilized. At each stage, high quality data sets are required.

A limitation of nested models is that a reasonable ratio should be maintained between the parent and the child domain resolutions. The seminal work of Spall and Holland (1991) indicates that a parentchild ratio of 3:1 gives the best results. Another conundrum of nesting models is the interpolation from the coarse to the fine grid and the lateral boundary conditions, which should at least be mass conserving (Oddo and Pinardi 2008).

The first large-scale regional forecasting attempt was carried out in the Tropical Pacific, an El Niño forecasting system (Cane et al. 1986), followed several years later by a Mediterranean Sea, mesoscale-permitting operational prediction system (Pinardi and Woods 2002; Pinardi et al. 2003) and several U. S. Navy regional systems for the Intra-Americans Seas (Ko et al. 2003a) and the North Pacific Ocean (Ko et al. 2003b).

### *a. The El Niño prediction system*

Predictions in the tropics originated from the need to forecast the impacts of El Niño on socio-economic activities such as agriculture and fisheries and to reduce the risk of natural disasters on land. From the 1960s and 1970s, dedicated observations in the tropical Pacific formed the basis for understanding the mechanisms that generate changes in the temperature, winds and currents of the tropical Pacific. In his book, El Niño, La Niña, and the Southern Oscillation, G. Philander describes El Niño as follows: "At present El Niño describes not a local seasonal current off the coast of Peru but the infrequent "anõs de abundancia" (fertile and abundant years) and the associated changes of the tropical Pacific and the global atmosphere. El Niño is that phase of the Southern Oscillation in which the

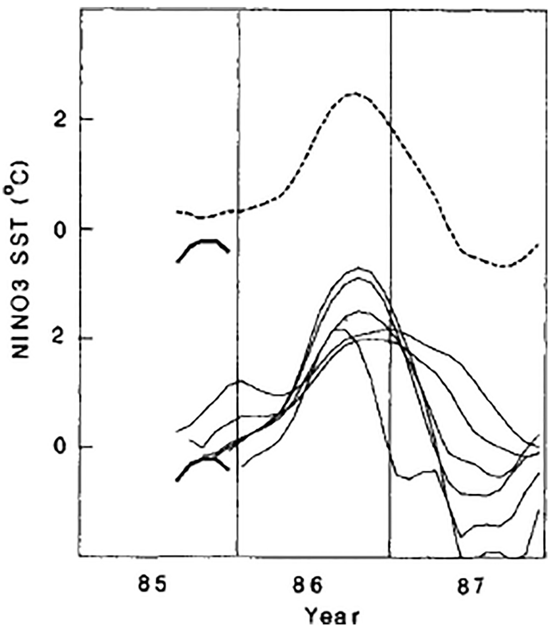


Figure 16. Forecast for 1986 of sea surface temperature anomalies (°C) in the NINO3 region. Light curves, values from forecasts initiated in the six successive months from August 1985 to January 1986. Dashed curve, average of the six forecasts; heavy curve, observed values. Reproduced from Cane et al. (1986).

trade winds are weak and where pressure is low over the eastern and high over the western tropical Pacific" (Philander 1989).

Coupled ocean and atmosphere numerical deterministic and statistical models were developed in the 1970s and 1980s. One of these models by Zebiak and Cane (1987) was used to issue the first successful forecast of El Niño conditions for the winter of 1986–1987 (Cane et al. 1986). The model was implemented in a tropical Pacific region between $\pm\, 29°\, N$, $S$ and from $124°\, E$ to $80°\, W$. The atmospheric model component was a steady-state linear shallow water model in the equatorial β-plane, devised by Gill (1980), and forced by Sea Surface Temperature (SST) anomalies and parameterized, low-level wind convergence. The ocean model component was a linear reduced gravity model in which the thermodynamics considered only temperature anomalies and the dynamics were driven by surface atmospheric wind stress.

The results of the first forecast carried out for the El Niño of 1986–1987 are shown in Figure 16. The forecast was successful because a major El Niño actually occurred in the winter of 1986–1987. The specific lesson from this historical prediction was that a specific, reduced complexity coupled ocean atmosphere model could be calibrated for El Niño forecasting, using El Niño events over the previous decade and specific process parameterizations. To some degree, this particular forecasting system was an advanced one, considering both a deterministic and a statistical learning approach to infer the parameterizations of the unresolved model processes.

It was soon evident that the predictability revealed by the coupled processes in the Pacific could be exploited to expand the forecasts to the seasonal range. Seasonal forecasts affect a variety of economic and social factors in a different way from the established short-term forecasts, and research started to investigate how the seasonal forecast information could be useful in the decision making process in both the public and private sectors. In 1994, the National Oceanographic and Atmospheric Administration (NOAA) established a pilot project that resulted in the establishment of a specialized institute, the International Research Institute for Climate and Society, the IRI (Goddard et al. 2014). The establishment of IRI and other similar institutions that followed demonstrates the growth of awareness for the use of climate forecasts in different economic and societal contexts. The IRI in fact was involved in efforts to reduce the impacts of seasonal and climate extremes in a number of ways, i.e., by improving assessment of risks using historical data on hazards and analyses of trends, by implementing and developing early warning systems informed by seasonal forecasts, and by developing index-based insurance products for financing and transfer of risk.

The IRI and a growing number of partners recognize that improved use of climate information represents an opportunity not only to reduce the impacts of extreme events today, but also to adapt to a warming climate whose impacts are likely to be felt most keenly in changes in the frequencies and intensities of hazards.

El Niño forecasting became operational only in the second half of the 1990s as a result of three major undertakings: 1) the Tropical Ocean Global Atmosphere observation system, which supported statistical studies of seasonal-to-interannual climate variability in the Pacific (McPhaden et al. 1998); 2) the development of global coupled ocean-atmosphere models and statistical models of varying complexity (Anderson et al. 1999), which revealed the sources of uncertainties and the barriers to predictability (Balmaseda et al. (1995) and Balmaseda 2017, this volume); and 3) the demonstration of the value of global ocean data assimilation systems to initialize coupled ocean forecasts (Derber and Rosati 1989; Saha et al. 2014).

### *b. The Mediterranean Sea basin-scale forecasting system*

In January 2000, the first ocean forecast for a regional ocean basin, the Mediterranean Sea, was issued and made available to the public. This first forecast system produced weekly 10-day forecasts that were disseminated two days after the nominal start of the forecast. Planning for the setup of the regional forecasting system had already appeared in the literature at the end of the 1990s (Horton et al. 1997; Pinardi and Flemming 1998) and practical implementation of the system was made possible by three major scientific and technological advancements (Pinardi et al. 2003; Pinardi and Coppini 2010):

1. The definition and implementation of a real-time satellite and *in situ* data collection and dissemination system. The *in situ* components considered subsurface measurements of temperature (Manzella et al. 2003). Satellite altimetry and sea surface temperatures were specifically analyzed for the Mediterranean Sea, and provided high-quality data for assimilation (Buongiorno Nardelli et al. 2003).
2. The development of a comprehensive data assimilation scheme that could assimilate the sea level anomaly from altimetry as well as the subsurface profiles (Demirov et al. 2003).
3. The calibration/validation of a primitive-equation, general circulation model in the entire Mediterranean Sea considering a parameterized connection with the Atlantic Ocean and air-sea interaction physics for momentum, heat and water one-way interactive fluxes (Castellari et al. 1998) which could properly simulate intense air-sea interaction processes producing specific water masses.

The key issue in achieving predictability in this region was to consider an appropriate open lateral boundary condition for the Gibraltar Strait, using the climatological knowledge of the Atlantic circulation available in the 1990s. The Gibraltar Strait was unresolved by the model grid, but with ad hoc choices of width and depth, the inflow/outflow at Gibraltar could be kept constant and realistic while specific water masses entering/exiting the basin were held fixed within an Atlantic box (Pinardi et al. 1997).

An analysis of RMSE for sea level anomalies in the Mediterranean Sea forecasting system from 1999 to 2010 is shown in Figure 17. Over the past 10 years, accuracy has increased by about 30% in the sea level anomaly RMSE and the improvement of the numerical model is the most important contributor to that increased performance. The requirement for more advanced numerical models will probably remain true for the next decade of ocean forecasting, because of the need to resolve mesoscale eddies, to improve the vertical viscosity and diffusivity parameterizations and the required coupling of surface wind waves with currents, the inclusion of tidal forcing and the complex parameterization of air-sea interactions.

### c. *Relocatable ocean forecasting systems*

Relocatable ocean models were used for real-time predictions of ocean mesoscale circulations for the first time in the Iceland-Faeroe Front region and in the Gulf of Mexico (Dietrich et al. 1993; Robinson et al. 1996). Perhaps somewhat earlier than the baroclinic mesoscale models, tidal and shallow water models (discussed in section 4) were developed with the concept of relocatability, again driven by multiple societal needs, especially navigation.

The initial version of the relocatable primitive equation model, part of the Harvard Ocean Prediction System (HOPS), was a rigid-lid model, initialized with the procedures described by Lozano et al. (1996) and Robinson et al. (1996). Subsequently, the relocatable HOPS and its improved versions were used for real-time forecasting and analysis of ocean dynamics

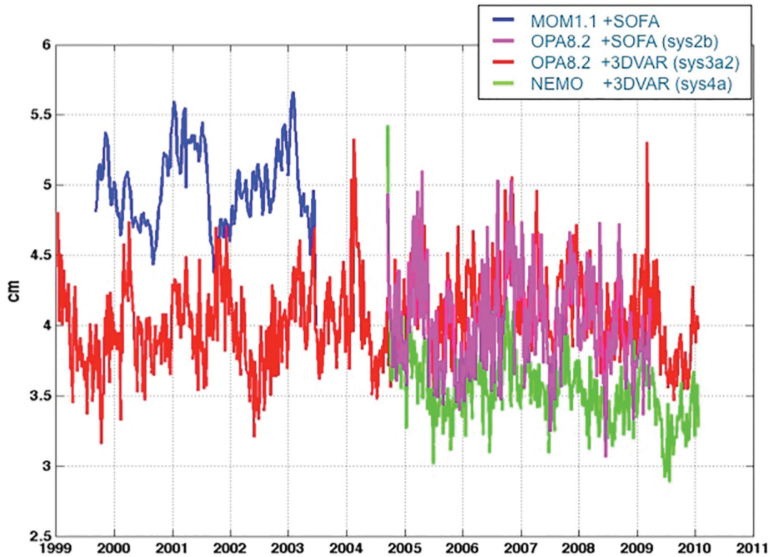


Figure 17. The root mean square error of the sea level anomaly misfits (difference between the model sea level and the satellite altimetric signal along the track) averaged over the basin surface for the years from 1999 to 2000 for different models and data assimilation systems. The blue line corresponds to the forecasting model given by the Modular Ocean Model (MOM) coupled with a reduced order Optimal Interpolation scheme. The purple line corresponds to a new model, the OPA general circulation model and the reduce order Optimal Interpolation. The red line corresponds to the change of the data assimilation to a 3Dvar system, and the green curve denotes a new model code, NEMO, and the same 3Dvar assimilation system.

in diverse regions of the world's oceans. Examples of applications occurred in the Atlantic Ionian Stream and Strait of Sicily region (Lermusiaux 1999; Robinson et al. 1999), the Strait of Gibraltar (Robinson and Sellschopp 2002), the Tunisia-Sardinia-Sicily region (Onken et al. 2003) and the Ligurian Sea (Robinson et al. 2002b). As discussed at the start of this section, the three phases of regional modeling and forecasting were exercised in these regions. As a result, regional modeling and forecasting were responsible for either explaining or discovering several ocean features and processes. In 1996, the first regional ocean forecasts using stochastic primitive equations with ensemble data assimilation were issued in real time for the Strait of Sicily (Lermusiaux 1999), using an advanced error subspace statistical estimation scheme (Lermusiaux et al. 2002; Lermusiaux 2006). The space and time variability of regional features in diverse regions was also quantified as part of the statistical dynamical predictions and analyses (Lermusiaux and Robinson 2001; Lermusiaux 2002).

Starting in the early 2000s, Maritime Rapid Environmental Assessment (MREA; Robinson and Sellschopp 2002) became one of the drivers of relocatable ocean modeling and forecasting. Such applications required a more rigorous evaluation of the model predictive capabilities (Robinson et al. 2002a) and few of such evaluations were completed in 2003 and 2004, for the relocatable Mini-HOPS modeling system applied to the Elba region and off the coast of Portugal (Leslie et al. 2008). Ko et al. (2008) also applied a relocatable modeling approach for MREA observations off the coast of Portugal.

Some of the relocatable models were used for direct societal applications. An example is the first regional ocean spill forecast for the Prestige oil spill in 2002, in collaboration with the Portuguese Navy (Lermusiaux et al. 2007). Relocatable models with data assimilation were also successfully used recently for studying Lagrangian dynamics and dispersion in the Gulf of Mexico region (Wei et al. 2016). Today, relocatable ocean models can be used both for emergency responses to oil spills (De Dominicis et al. 2014) and for fundamental studies of ocean dynamics, given the capability of multiple nesting and a resolution of a few hundred meters in both coastal and open ocean areas. One of the most advanced relocatable systems is the RELO (RELOcatable) ocean nowcast/forecast system, used by the U. S. Navy in numerous locations around the global ocean (Clark and Mask 2014). A new relocatable system with unstructured grid model capabilities has also been developed recently (Trotta et al. 2016).

Critical to all of these regional and relocatable models are the methods for downscaling and nesting of different regional models (e.g., Onken et al. 2005; Lermusiaux et al. 2011; Ramp et al. 2011). For a review of nesting schemes, we refer to Debreu and Blayo (2008), Oddo and Pinardi (2008), and Mason et al. (2010). Because the original HOPS was a rigid-lid model, a new conservative, finite-volume, structured ocean model code was developed with implicit two-way nesting for multiscale, hydrostatic primitive equation dynamics with a nonlinear free-surface (Haley and Lermusiaux 2010). This multidisciplinary simulation, estimation and assimilation system includes the following regional modeling capabilities: balanced and nested initialization and downscaling (Haley et al. 2013); multi-resolution, data-assimilative tidal prediction and inversion (Logutov and Lermusiaux 2008); fast-marching coastal objective analysis (Agarwal and Lermusiaux 2011), stochastic subgrid-scale models (e.g., Lermusiaux 2006) and data assimilation and adaptive sampling (Lermusiaux 2007). For multiple physics and timescales, combinations of implicit two-way nesting with optimized initialization and downscaling schemes (Haley et al. 2015) are very useful for insuring consistency among model fields and reduce non-physical transients due to the nesting of multiple model types.

## 7. Global ocean predictions

Global ocean predictions started in the 1990s in the US and Europe, although the planning for global ocean prediction systems had been in place at the US Office of Naval Research since the 1980s (Peloquin 1992).

The problem of global ocean forecasting, even for the shortest lead time, involves the problem of properly interfacing the atmospheric heat, water and momentum fluxes and sea ice. The first ocean forecast, described in section (5.b), did not use atmospheric forcing because it was centered around the deep thermocline ocean field, where the influence of atmospheric forcing is felt on time scales longer than a week. In contrast, global ocean forecasting concentrates on upper mixed-layer dynamics, which, in turn, implies adequate atmospheric forcing and vertical as well as horizontal subgrid-scale parameterizations. The success of the El Niño forecast in section (6.a) was due to the proper account of air-sea exchange processes, and a method needed to be formulated to achieve uncoupled global ocean predictions. The landmark paper of Rosati and Miyakoda (1988) defined the first complete set of physical parameterizations of air-sea interactions to run an uncoupled global ocean model in forecasting mode. The model was a $1 \times 1°$ global model with $1/3 \times 1/3°$ grid refinement in the tropical regions, and it showed that the atmospheric forcing frequency had to be hourly to achieve realistic sea surface temperature fields. Even if the results were eddy resolving only at the tropics, the conclusion is that uncoupled ocean forecasting requires a high-frequency, atmospheric forecast forcing, and atmospheric forecast uncertainties are an important component of the limited predictability in the oceanic upper water column (Pinardi et al. 2011).

In the 1980s and early 1990s, the problem of global ocean predictions was solved by partitioning the problem into simpler, more affordable sub-components. The water column was generally considered to be composed of a mixed-layer dynamical portion and subsurface geostrophic and sea ice subsystems, each described by a different set of weakly coupled prognostic equations. The initial suite of oceanographic models and products from the Fleet Numerical Oceanography Center (Clancy 1992; Clancy and Sadler 1992) was composed of mixed-layer models, geostrophic flow-field diagnostic computations and several statistical interpolation/extrapolation data assimilation schemes. In the same way, sea ice predictions were defined as separate forecasting problems to achieve a reasonable degree of predictability of sea ice thickness and drift (Preller 1992).

The development of global ocean short-term predictions was initially hampered by the need for mesoscale resolution models and, thus, global models with grid spacing larger than approximately $1/8°$. Mesoscale variability is so pervasive that without such eddy-resolving models, accuracy would be low and it would be very difficult to assimilate the sea level from satellite altimetry to increase the forecast accuracy (Wunsch 2002). Reanalyses are possible even at coarser resolutions because data assimilation filters are used in smoothing mode, but ocean models need to be eddy resolving if the aim is to accurately predict the mixed-layer structures and variability.

The first global ocean forecasting systems with global data assimilation components became operational at the end of the 1990s. The Forecasting Ocean Assimilation Model (FOAM) (Bell et al. 2000) became the first operational global ocean prediction system in 1997 but it was run at a $1°$ horizontal resolution and as such was non-eddy resolving. The requirements for global scale mesoscale resolving models ($\lesssim 1/10°$) have been difficult to satisfy because of limited available computer resources. At the beginning of the 21st century, different groups tried solving this resource problem in different ways.

The French global Mercator operational system began running in October 2005 at 1/4° horizontal resolution (eddy permitting) with 46 vertical levels (Bahurel et al. 2006). The Australian global operational BLUElink system began running operationally in 2007 using the Modular Ocean Model (MOM; Griffies 2010) at a variable horizontal grid resolution of approximately 1/10° around Australia and decreasing to 2° at other locations, and using 47 vertical levels (Schiller and Smith 2006). The U. S. Navy took a different approach in the first decade of the 21st century by running two global ocean models that defined one global ocean forecast system. A 7-layered ocean model (the Navy Layered Ocean Model; NLOM) ran at high resolutions (1/16°–1/32°) to optimize the assimilation of along-track satellite altimetry and satellite SST data and to generate synthetic temperature and salinity profiles. These profiles were then assimilated into a coarser (1/8°) horizontal resolution global ocean model (Navy Coastal Ocean Model; NCOM) with 40 vertical layers. This two-component system required fewer computational resources than a single global model with high horizontal and vertical resolution (Rhodes et al. 2002; Hurlburt et al. 2008).

As computational resources have grown, so has the operational community's ability to predict the global ocean at higher resolutions. The current BLUElink operational system uses a 10-km horizontal grid resolution around Australia but is extending that resolution globally. The Mercator global ocean prediction system now runs operationally at 1/12° horizontal resolution. The U. S. Navy, using the Hybrid Coordinate Ocean Model (HYCOM) coupled with the Los Alamos Community Ice CodE (CICE), runs a daily global operational prediction using 1/12° degree horizontal resolution and 41 hybrid vertical layers in the ocean. These operational systems also make use of the most advanced data assimilation techniques, including variational data assimilation (Lorenc et al. 2000), Kalman filters and Ensemble techniques (Evensen 2003). A new, pre-operational system was just developed in Italy with a 1/16° resolution model (Iovino et al. 2016) and a 3Dvar assimilation system (Storto et al. 2011). Tonani et al. (2015) discuss the development and status of a number of existing global ocean forecasting systems.

## 8. Discussion

In this paper, we have reviewed the development of atmospheric predictions and ocean predictions for waves, storm surges and deep currents from an historical point of view. Bauer et al. (2015) defined numerical weather prediction as a "quiet revolution" that nevertheless generated a leap in knowledge as fundamental as the predictions of the basic constituents of matter.

Predictions allow the verification of the "theory" of the atmosphere and the ocean by observation of the natural world. In oceanography and meteorology, one of the methods of verification of theories is achieved by numerical predictions. In other words, the theoretical framework for understanding the variability and structure of the oceans and atmosphere uses numerical predictions as a tool, through which predictions can be compared with and thus verified by observations. For the ocean, this fundamental step in knowledge did not take place until the 1980s.

The science of predictions is indeed a unique framework on which to verify theories using observations. Charney et al. (1950) and Robinson et al. (1984) understood the importance of this situation and carried out the two first forecast experiments to verify the atmospheric and oceanic fundamental equations of motion. They also foresaw the numerous practical implications of such discoveries that have such an effect on our lives today.

Operational meteorological and oceanographic centers continue to apply the method of comparing numerical predictions to observations. They produce the basic data sets on which new theories of atmospheric and oceanic phenomena are developed and numerical models are improved in their representation of realistic natural processes. Examples of new theories are the Lorenz theory of atmospheric predictability, based upon the study of atmospheric forecasts (Lorenz 1982); the mixed baroclinic/barotropic ocean instability processes (Pinardi and Robinson 1986), giving rise to the Gulf Stream ring pinch off (Robinson et al. 1988) and to the meandering of oceanic frontal systems (Spall 1989; Liang and Robinson 2004) based on oceanic analyses.

Numerical models and observations allow advances in the theory of natural oceanographic and meteorological phenomena, using a sequential refinement method whereby the numerical models are gradually modified as they learn from comparing their predictions with observations. At the same time, observation networks are developed to better meet the needs of numerical models to resolve natural processes.

The concept of theory refinement in incremental steps using observations is not actually new, and can easily be connected to the least square method discussed by Gauss (1809). As described by Sorenson (1970), the least square method was developed to solve the problem of planetary motion. In astronomy as well as in meteorology and oceanography, phenomena have an intrinsic time-dependent nature and observations of the phenomena of interest are not sampled adequately at all space and time scales. As Gauss and Davis stated (Gauss and Davis 2004):

> "…[S]ince our measurements and observations are nothing more than approximations of the truth, the same must be true of all calculations resting upon them, and the highest aim of all computations made concerning concrete phenomena must be to approximate, as nearly as practicable, the truth. But this can be accomplished in no other way than by a suitable combination of more observations than the number absolutely required for the determination of the unknown quantities. This problem can only be undertaken when an approximate knowledge of the orbit has been already attained, which is later to be corrected so as to satisfy all the observations in the most accurate manner possible."

This fundamental statement, which rests on the solid mathematical framework developed by Gauss and later by Kalman (1963), puts into perspective the problem of estimating the natural variables $\mathbf{x}$ in (1) by assuming that they are all affected by errors, i.e.,

$$\mathbf{x} = \mathbf{x}_t + \epsilon_{\mathbf{x}} \tag{7}$$

in both observations and models. In (7), $\mathbf{x}_t$ is the truth that is contained in our theories and measurements but that we can only know with a certain amount of error.

It is evident that present and future research in ocean and atmospheric predictions focuses on understanding the sources of uncertainties or "errors" in the numerical models. In ocean predictions, the main sources of uncertainties can be summarized in five categories: 1) errors in the initial conditions due to a lack of observations to correct the model's first guess; 2) errors in the forcing functions, including the atmospheric (with momentum, heat and water fluxes) and land (including river runoff) forcings; 3) the physics of the numerical model and its numerical approximations, the coupling with surface waves and especially the physics and thermodynamics of sea ice and water-ice coupling; 4) the internal feedback between the marine ecosystem and the physical environment, including subsurface optics, drag coefficients, among others, and 5) knowledge of bathymetry and its time variability, including sediment deposition and resuspension.

It took more than 60 years for meteorology to achieve reasonably accurate predictions (see Fig. 1). Learning from the experiences and problems solved in meteorology, ocean predictions might achieve reasonable accuracy within 40–50 years from their start, that is, within the next decade. Reasonable accuracy is here intended to mean "usable" accuracy, as it was defined by Hollingsworth et al. (1980) on the basis of synoptic evaluation of each individual case. The requirements for understanding the limits of ocean predictability are heavy, because *in situ* observations are difficult to maintain and observational techniques need to be inter-calibrated, data assimilation schemes require a very good knowledge of multi-variate error statistics and the computational requirements of numerical models are constantly increasing. The challenges are even greater if we consider that future ocean forecast systems are moving toward truly coupled (atmosphere-ocean-wave-ice-hydrology-land-ecosystem) models. This is true both for global and regional predictions. Moreover, longer lead-time predictions are now being formulated from the seasonal to the multi-decadal timescales for regional areas and the globe.

The problem cannot be properly tackled without international cooperation in the field of ocean sciences and operational services. The most important international groups involved in the development of modeling and observational strategies for ocean predictions are the Global Ocean Data Assimilation Experiment (Dombrowsky et al. 2008), which brings together the forecasting community to advance numerical models; the Global Ocean Observing System (Summerhayes 2002), which develops *in situ* observations and networks; and the Group of Earth Observations (Plag 2008), which develops the satellite part of the observation system.

From the operational side, for both observations and models, the Joint Committee of Oceanography and Marine Meteorology (JCOMM) (http://www.jcomm.info/) brings together operational real-time observation networks and weather and climate forecasting centers across meteorology and oceanography. All of this work seems to suggest that over the upcoming decade, 2020–2030, the science of ocean predictions will be consolidated and other challenges such as climate predictions and projections will be solved, finally bringing society the benefits of the fundamental methodological developments of the past 60 years.

**Appendix A**

Quasigeostrophic dynamical equations derive from the primitive equations using a field perturbation expansion in the so-called Rossby number. The latter is the ratio between the earth rotation day length and the flow field time scale. The perturbation expansion works as far as this number is small, i.e. the flow field time scale is longer than a day. For the ocean mesoscales the time scale is of the order of few weeks and the Rossby number is $10^{-2}$. The baroclinic quasigeostrophic equations used for the first real-time ocean forecast (Robinson et al. 1986) were written as:

$$\left[\frac{\partial}{\partial t} + \alpha J(\psi, )\right]\left\{\nabla^2\psi + \beta y + \frac{\partial}{\partial z}\left[\Gamma^2 \frac{\partial}{\partial z}(\sigma\psi)\right]\right\} = F \tag{8}$$

where

1. $\vec{v} = \hat{k} \times \vec{\nabla}\psi$ is the geostrophic velocity field $\psi$ is the streamfunction and $\hat{k}$ is the unit vector in the vertical direction;
2. $\beta = \beta_0 t_0 d$ is the $\beta$-scale factor measuring the relative size of planetary versus relative vorticity advection;
3. $\alpha = \frac{t_0 V_0}{d}$ is the nonlinear scale factor and $t_0$ is the scaling time, $V_0$ is the velocity scale and $d$ is the horizontal space scale;
4. $\Gamma^2 = \frac{f_0^2 d^2}{N_0^2 H^2}$ is the stretching or baroclinicity factor, where $f_0$ is the representative Coriolis parameter, $N_0$ is a representative Brünt-Väïsälä frequency value and $H$ is the vertical scale;
5. $\sigma = \frac{N_0^2}{N^2(z)}$ where $N^2(z)$ is the mean Brünt-Väïsälä frequency profile for the area of interest;
6. $J(\psi, ) = \frac{\partial\psi}{\partial x}\frac{\partial}{\partial y} - \frac{\partial\psi}{\partial y}\frac{\partial}{\partial x}$ is the Jacobian operator or geostrophic advection;
7. $F$ is the representation of different dissipative processes by a Shapiro filter (Shapiro 1971);
8. $\nabla^2\psi + \frac{\partial}{\partial z}\left[\Gamma^2 \frac{\partial}{\partial z}(\sigma\psi)\right]$ is called the dynamic vorticity, sum of the relative and thermal vorticity, respectively.

For the 1983 California current experiment, (8) was used with all of the terms and a specific choice of nondimensional parameters $\alpha$, $\beta$ and $\Gamma^2$. In the case of the Charney et al. (1950) atmospheric forecast, the model was barotropic, i.e., $\Gamma^2 = 0$ and $F = 0$. The authors themselves realize that the neglected baroclinicity is a major source of uncertainty for the forecast.

*Acknowledgments.* The authors would like to thank the anonymous reviewers for comments that greatly improved the original manuscript. Section 4 draws mainly on Cartwright (1999) and Pugh and Woodworth (2014). Dr. Kevin Horsburgh and Roger Flather are thanked for literature suggestions.

REFERENCES

Abbe, C. 1901. The physical basis of long-range weather forecasts 1. Mon. Weather Rev., *29*(12), 551–561. doi: 10.1175/1520-0493(1901)29[551c:TPBOLW]2.0.CO;2

Abdalla, S., and E. Özhan. 1993. Third-generation wind-wave model for use on personal computers. J. Waterw. Port Coast. Ocean Eng., *119*(1), 1–14. doi: 10.1061/(ASCE)0733-950X(1993)119:1(1)

Adam, Y. 1979. Belgian real-time system for the forecasting of currents and elevations in the North Sea. Marine Forecasting Predictability and Modelling in Ocean Hydrodynamics, Proceedings of the 10th International Liége Colloquium on Ocean Hydrodynamics, Elsevier Oceanography Series, vol. 25, C. J. Nihoul, ed. New York: Elsevier Science, 411–425. doi: 10.1016/S0422-9894(08)71141-3

Agarwal, A., and P. F. Lermusiaux. 2011. Statistical field estimation for complex coastal regions and archipelagos. Ocean. Model., *40*(2), 164–189.

Amin, M. 1982. On analysis and forecasting of surges on the west coast of Great Britain. Geophys. J. Int., *68*(1), 79–94. doi: 10.1111/j.1365-246X.1982.tb06963.x

Anderson, J., H. van den Dool, A. Barnston, W. Chen, W. Stern, and J. Ploshay. 1999. Present-day capabilities of numerical and statistical models for atmospheric extratropical seasonal simulation and prediction. Bull. Am. Meteorol. Soc., *80*(7), 1349–1361. doi: 10.1175/1520-0477

Ardhuin, F., E. Rogers, A. V. Babanin, J.-F. Filipot, R. Magne, A. Roland, A. Van Der Westhuysen, et al. 2010. Semiempirical dissipation source functions for ocean waves. Part i: Definition, calibration, and validation. J. Phys. Oceanogr., *40*(9), 1917–1941. doi: 10.1175/2010JPO4324.1

Arns, A., T. Wahl, S. Dangendorf, and J. Jensen. 2015. The impact of sea level rise on storm surge water levels in the northern part of the German Bight. Coast. Eng., *96*, 118–131. doi: 10.1016/j.coastaleng.2014.12.002

Bahurel, P., and MERCATOR PROJECT TEAM. 2006. Mercator ocean global to regional ocean monitoring and forecasting, *in Ocean Weather Forecasting*, New York: Springer, 381–395. doi: 10.1007/1-4020-4028-8_14

Balmaseda, M. A., M. K. Davey, and D. L. T. Anderson. 1995. Decadal and seasonal dependence of enso prediction skill. J. Clim., *8*(11), 2705–2715. doi: 10.1175/1520-0442

Bauer, P., A. Thorpe, and G. Brunet. 2015. The quiet revolution of numerical weather prediction. Nature, *525*(7567), 47–55. doi: 10.1038/nature14956

Bell, M. J., R. M. Forbes, and A. Hines. 2000. Assessment of the {FOAM} global data assimilation system for real-time operational ocean forecasting. J. Mar. Syst., *25*(1), 1–22. doi: 10.1016/S0924-7963(00)00005-1

Berry, P., and J. Marshall. 1989. Ocean modelling studies in support of altimetry. Dyn. Atmos. Oceans, *13*(3–4), 269–300. doi: 10.1016/0377-0265(89)90042-0

Bertotti, L., J.-R. Bidlot, C. Bunney, L. Cavaleri, L. Delli Passeri, M. Gomez, J.-M. Lefèvre, et al. 2012. Performance of different forecast systems in an exceptional storm in the western mediterranean sea. Q. J. R. Meteorol. Soc., *138*(662), 34–55. doi: 10.1002/qj.892

Bjerknes, V. 1904. Das problem der wettervorhersage: betrachtet vom standpunkte der mechanik und der physik. Physik. Met. Zeit., *21*, 1–7.

Bjerknes, V. 1914. Meteorology as an exact science 1. Mon. Weather Rev., *42*(1), 11–14. doi: 10.1175/1520-0493(1914)42<11:MAAES>2.0.CO;2

Booij, N., R. Ris, and L. H. Holthuijsen. 1999. A third-generation wave model for coastal regions: 1. Model description and validation. J. Geophys. Res. Oceans, *104*(C4), 7649–7666. doi: 10.1029/98JC02622

Bretherton, F. P., R. E. Davis, and C. Fandry. 1976. A technique for objective analysis and design of oceanographic experiments applied to mode-73. Deep-Sea Res. Oceanogr. Abstr., *23* (7), 559–582. doi: 10.1016/0011-7471(76)90001-2

Brown, J. M., R. Bolaños, and J. Wolf. 2013. The depth-varying response of coastal circulation and water levels to 2D radiation stress when applied in a coupled wave–tide–surge modelling system during an extreme storm. Coast. Eng., *82*, 102–113. doi: 10.1016/j.coastaleng.2013.08.009

Buongiorno Nardelli, B., G. Larnicol, E. D'Acunzo, R. Santoleri, S. Marullo, and P. Y. Le Traon. 2003. Near real time SLA and SST products during 2-years of mfs pilot project: Processing, analysis of the variability and of the coupled patterns. Ann. Geophys., *21*(1), 103–121. doi: 10.5194/angeo-21-103-2003

Cane, M. A., S. Zebiak, and S. Dolan. 1986. Experimental forecasts of el niño. Nature, *321*, 827–832. doi: 10.1038/321827a0

Cardone, V. J., W. J. Pierson, and E. G. Ward. 1975. Hindcasting the Directional Spectra of Hurricane Generated Waves. Offshore Technology Conference. doi: 10.4043/2332-MS

Carnes, M. R., J. L. Mitchell, and P. W. Witt. 1990. Synthetic temperature profiles derived from geosat altimetry: Comparison with air-dropped expendable bathythermograph profiles. J. Geophys. Res. Oceans, *95*(C10), 17979–17992. doi: 10.1029/JC095iC10p17979

Carter, E. F., and A. R. Robinson. 1987. Analysis models for the estimation of oceanic fields. J. Atmos. Ocean. Technol., *4*(1), 49–74. doi: 10.1175/1520-0426(1987)004<0049:AMFTEO>2.0.CO;2

Carton, J. A. 1987. How predictable are the geostrophic currents in the recirculation zone of the north atlantic? J. Phys. Oceanogr., *17*(6), 751–762. doi: 10.1175/1520-0485(1987)017<0751:HPATGC>2.0.CO;2

Cartwright, D. 1999. Book review: Tides: A scientific history/cambridge u press, 1998. J. Br. Astron. Assoc., *109*, 291.

Castellari, S., N. Pinardi, and K. Leaman. 1998. A model study of air–sea interactions in the mediterranean sea. J. Mar. Syst., *18*(1), 89–114. doi: 10.1016/S0924-7963(98)90007-0

Cavaleri, L., A. Benetazzo, F. Barbariol, J.-R. Bidlot, and P. A. E. M. Janssen. 2017. The draupner event: The large wave and the emerging view. Bull. Am. J. Meteorol. Soc., *98* (4), 729–735. doi: 10.1175/BAMS-D-15-00300.1

Cavaleri, L., L. Bertotti, and J.-R. Bidlot. 2015. Waving in the rain. J. Geophys. Res. Oceans, *120*(5), 3248–3260. doi: 10.1002/2014JC010348

Charney, J. 1955. The use of the primitive equations of motion in numerical prediction. Tellus, *7*(1), 22–26. doi: 10.1016/S0924-7963(98)90007-0

Charney, J. G. 1948. On the scale of atmospheric motions. Geofysiske Publikasjoner, *17*(2), 251–265.

Charney, J. G., R. Fjortoft, and J. Von Neumann. 1950. Numerical integration of the barotropic vorticity equation. Tellus, *2*(4), 237–254. doi: 10.1111/j.2153-3490.1950.tb00336.x

Chen, C., R. C. Beardsley, R. A. Luettich, J. J. Westerink, H. Wang, W. Perrie, Q. Xu, et al. 2013. Extratropical storm inundation testbed: Intermodel comparisons in scituate, Massachusetts. J. Geophys. Res. Oceans, *118*(10), 5054–5073. doi: 10.1002/jgrc.20397

Clancy, R. 1992. Operational modeling: Ocean modeling at the fleet numerical oceanography center. Oceanography, *5*(1), 31–35. doi: 10.5670/oceanog.1992.29

Clancy, R., and W. Sadler. 1992. The fleet numerical oceanography center suite of oceanographic models and products. Weather Forecast., *7*(2), 307–327. doi: 10.1175/1520-0434(1992)007<0307:TFNOCS>2.0.CO;2

Clark, R., and A. Mask. September 2014. Regional and coastal prediction with the relocatable ocean nowcast/forecast system. Oceanography, *27*(3), 44–55. doi: 10.5670/oceanog.2014.67

Courant, R., K. Friedrichs, and H. Lewy. 1967. On the partial difference equations of mathematical physics. IBM J. Res. Dev., *11*(2), 215–234. doi: 10.1147/rd.112.0215

Cushman-Roisin, B., and J.-M. Beckers. 2011. *Introduction to Geophysical Fluid Dynamics: Physical and Numerical Aspects*, vol. 101 (2nd ed.). New York: Academic Press.
Daley, R. 1991. Atmospheric Data Analysis, Cambridge Atmospheric and Space Science Series, vol. 6966. Cambridge: Cambridge University Press, 25.
Darwin, G. H. 1883. Report of a Committee for the Harmonic Analysis of Tidal Observations. London: British Association for the Advancement of Science.
Davies, A., and R. Flather. 1987. Computing extreme meteorologically induced currents, with application to the northwest european continental shelf. Continental Shelf Research, *7*(7), 643–683.
De Dominicis, M., S. Falchetti, F. Trotta, N. Pinardi, L. Giacomelli, E. Napolitano, L. Fazioli et al. 2014. A relocatable ocean model in support of environmental emergencies. Ocean Dyn., *64*(5), 667–688. doi: 10.1007/s10236-014-0705-x
De Mey, P., and A. R. Robinson. 1987. Assimilation of altimeter eddy fields in a limited-area quasi-geostrophic model. J. Phys. Oceanogr., *17*(12), 2280–2293. doi: 10.1175/1520-0485(1987)017<2280:AOAEFI>2.0.CO;2
de Vries, H., M. Breton, T. de Mulder, Y. Krestenitis, R. Proctor, K. Ruddick, J. C. Salomon, et al. 1995. A comparison of 2d storm surge models applied to three shallow european seas. Environ. Softw, *10*(1), 23–42. doi: 10.1016/0266-9838(95)00003-4
Debreu, L., and E. Blayo. 2008. Two-way embedding algorithms: A review. Ocean Dyn., *58*(5–6), 415–428. doi: 10.1007/s10236-008-0150-9
Defant, A. 1961. *Physical Oceanography, vol. 2*. Oxford: Pergamon press.
Demirov, E., N. Pinardi, C. Fratianni, M. Tonani, L. Giacomelli, and P. De Mey. 2003. Assimilation scheme of the mediterranean forecasting system: Operational implementation. Ann. Geophys., *21*(1), 189–204. doi: 10.5194/angeo-21-189-2003
Derber, J., and A. Rosati. 1989. A global oceanic data assimilation system. J. Phys. Oceanogr., *19*(9), 1333–1347. doi: 10.1175/1520-0485
Dewitt, P. 1987. Modal decomposition of the monthly gulf stream/kuroshio temperature fields. Naval Oceanographic Office Tech. Rep, *298*. Stennis Space Center, MS: Naval Oceanographic Office. 40 pp.
Dietrich, D. E., D.-S. Ko, and L. A. Yeske. 1993. On the application and evaluation of the relocatable diecast ocean circulation model in coastal and semi-enclosed seas. Technical report, DTIC Document. Starkville, MS: Mississippi State University Center for Air Sea Technology.
Dixon, M. J., and J. A. Tawn. 1992. Trends in uk extreme sea-levels: A spatial approach. Geophys. J. Int., *111*(3), 607–616. doi: 10.1111/j.1365-246X.1992.tb02115.x
Dobricic, S., and N. Pinardi. 2008. An oceanographic three-dimensional variational data assimilation scheme. Ocean Model., *22*(3), 89–105. doi: 10.1016/j.ocemod.2008.01.004
Dombrowsky, E., L. Bertino, G. Brassington, E. Chassignet, F. Davidson, H. Hurlburt, M. Kamachi, et al. 2008. Godae systems in operation. Oceanography, *22*(3), 80–95. doi: 10.5670/oceanog.2009.68
Doodson, A. T. 1921. The harmonic development of the tide-generating potential. Proc. R. Soc. Lond. A, *100*(704), 305–329. doi: 10.1098/rspa.1921.0088
Dronkers, J. 1969. Tidal computations for rivers, coastal areas, and sea. J. Hydraul. Div., *95*(1), 29–78.
Dube, S., I. Jain, A. Rao, and T. Murty. 2009. Storm surge modelling for the bay of bengal and arabian sea. Nat Hazards, *51*(1), 3–27. doi 10.1007/s11069-009-9397-9
Edwards, P. N. 2010. Computer Models, Climate Data, and the Politics of Global Warming. Cambridge, MA: MIT Press.
Epstein, E. S. 1969. Stochastic dynamic prediction. Tellus, *21*(6), 739–759. doi: 10.1111/j.2153-3490.1969.tb00483.x
Evensen, G. 2003. The ensemble kalman filter: Theoretical formulation and practical implementation. Ocean Dyn., *53*(4), 343–367. doi: 10.1007/s10236-003-0036-9

Ewing, J. 1971. A numerical wave prediction method for the north atlantic ocean. Deutsch. Hydrogr. Z., *24*(6), 241–261. 10.1007/BF02225707

Farrell, W. 1973. Earth tides, ocean tides and tidal loading. Philos. Trans. R. Soc Lond. A, *274*(1239), 253–259. doi: 10.1098/rsta.1973.0050

Flather, R. 1976. A tidal model of the northwest european continental shelf. Mem. Soc. R. Sci. Liege, *10*(6), 141–164. doi: 10.1029/2006JC003531

Flather, R. 1979. Recent results from a storm surge prediction scheme for the North Sea. Elsevier Oceanogr. Ser., *25*, 385–409. doi: 10.1016/S0422-9894(08)71140-1

Flather, R. 1987. Estimates of extreme conditions of tide and surge using a numerical model of the north-west european continental shelf. Estuar. Coast. Shelf Sci., *24*(1), 69–93. doi: 10.1016/0272-7714(87)90006-0

Flather, R. 2001. Storm surges, *in* Encyclopedia of Ocean Sciences, J. Steele, K. Turekian, and S. Thorpe, eds. London: Academic Press, 2882–2892.

Flather, R., and A. Davies. 1976. Note on a preliminary scheme for storm surge prediction using numerical models. Q. J. R. Meteorol. Soc., *102*(431), 123–132. doi: 10.1002/qj.49710243110

Flather, R. A. 2000. Existing operational oceanography. Coast. Eng., *41*(1), 13–40. doi: 10.1016/S0378-3839(00)00025-9

Flowerdew, J., K. Horsburgh, C. Wilson, and K. Mylne. 2010. Development and evaluation of an ensemble forecasting system for coastal storm surges. Q. J. R. Meteorol. Soci., *136*(651), 1444–1456.

Flowerdew, J., K. Mylne, C. Jones, and H. Titley. 2013. Extending the forecast range of the uk storm surge ensemble. Q. J. R. Meteorol. Soc., *139*(670), 184–197.

Gallet, B., and W. R. Young. 2014. Refraction of swell by surface currents. J. Mar. Res., *72*(2), 105–126.

Gandin, L. S. 1965. Objective Analysis of Meteorological Fields (Obektivnyi Analiz Meteorologicheskikh Polei). Jerusalem: Israel Program for Scientific Translation.

Gauss, C. F. 1809. Theoria motus corporum coelestium in sectionibus conicis solem ambientium. Hamburgi Sumtibus Frid. Perthes et I.H.Besser (Publisher).

Gauss, C. F., and C. H. Davis. 2004. Theory of the Motion of the Heavenly Bodies Moving about the Sun in Conic Sections. Boston: Little, Brown.

Gelci, R., H. Cazalé, and J. Vassal. 1957. Prévision de la houle. la méthode des densités spectroangulaires. Bulletin d'information du Comité d'Océanographie et d'Etude des Côtes, *9*, 416–435.

Gilchrist, B., and G. P. Cressman. 1954. An experiment in objective analysis. Tellus, *6*(4), 309–318. doi: 10.1111/j.2153-3490.1954.tb01126.x

Goddard, L., W. E. Baethgen, H. Bhojwani, and A. W. Robertson. 2014. The International Research Institute for Climate and Society: Why, what and how. Earth Perspectives, *1*(1–10), Springer, doi: 10.1186/2194-6434-1-10

Greenspan, H. P. 1956. The generation of edge waves by moving pressure distributions. J. Fluid Mech., *1*(06), 574–592. doi: 10.1017/S002211205600038X

Griffies, S. 2010. Elements of MOM4p1. Princeton: NOAA/Geophysical Fluid Dynamics Laboratory.

Gunther, H., W. Rosenthal, T. Weare, B. Worthington, K. Hasselmann and J. Ewing. 1979. A hybrid parametrical wave prediction model. J. Geophys. Res., Oceans, *84*(C9), 5727–5738. doi: 10.1029/JC084iC09p05727

Haley, P. J., and P. F. Lermusiaux. 2010. Multiscale two-way embedding schemes for free-surface primitive equations in the "multidisciplinary simulation, estimation and assimilation system." Ocean Dyn., *60*(6), 1497–1537. doi: 10.1007/s10236-010-0349-4

Hansen, W. 1956. Theorie zur errechnung des wasserstandes und der strömungen in randmeeren nebst anwendungen1. Tellus, *8*(3), 287–300.

Harris, R. A. 1904. Manual of Tides (Part IVB) Cotidal Lines of the World. Washington, D.C.: Department of Commerce and Labor, Coast and Geodetic Survey.

Hasselmann, K. 1962. On the non-linear energy transfer in a gravity-wave spectrum part 1. General theory. J. Fluid Mech., *12*(04), 481–500. doi: 10.1017/S0022112062000373

Hasselmann, K., T. Barnett, E. Bouws, H. Carlson, D. Cartwright, K. Enke, J. Ewing et al. 1973. Measurements of wind-wave growth and swell decay during the joint North Sea wave project (JONSWAP). Technical report, Hamburg: Deutches Hydrographisches Institut.

Hasselmann, S., K. Hasselmann, J. Allender, and T. Barnett. 1985. Computations and parameterizations of the nonlinear energy transfer in a gravity-wave specturm. Part ii: Parameterizations of the nonlinear energy transfer for application in wave models. J. Phys. Oceanogr., *15*(11), 1378–1391. doi: 10.1175/1520-0485(1985)015<1378:CAPOTN>2.0.CO;2

Hasselmann, K., W. Sell, D. Ross, and P. Müller. 1976. A parametric wave prediction model. J. Phys. Oceanogr., *6*(2), 200–228. doi: 10.1175/1520-0485(1976)006<0200:APWPM>2.0.CO;2

Heaps, N. S. 1969. A two-dimensional numerical sea model. Philos. Trans. R. Soc. Lond. A, *265*(1160), 93–137. doi: 10.1098/rsta.1969.0041

Hendershott, M. 1972. The effects of solid earth deformation on global ocean tides. Geophys. J. Int., *29*(4), 389–402. doi: 10.1111/j.1365-246X.1972.tb06167.x

Hill, G. 1968. Grid telescoping in numerical weather prediction. J. Appl. Meteorol., *7*(1), 29–38. doi: 10.1175/1520-0450(1968)007<0029:GTINWP>2.0.CO;2

Hollingsworth, A. 1980. An experiment in Monte Carlo forecasting, *in* Proceedings of WMO Symposium on Probabilistic and Statistical Methods in Weather Forecasting (8–12 September 1980; Nice, France). 65–85.

Hollingsworth, A., K. Arpe, M. Tiedtke, M. Capaldo, and H. Savijärvi. 1980. The performance of a medium-range forecast model in winter–impact of physical parameterizations. Mon. Weather Rev., *108*(11), 1736–1773. doi: 10.1175/1520-0493(1980)108<1736:TPOAMR>2.0.CO;2

Holton, J. R., and G. J. Hakim. 2012. *An Introduction to Dynamic Meteorology*, vol. 88. New York: Elsevier Science.

Horsburgh, K., and H. De Vries. 2011. Guide to Storm Surge Forecasting. Geneva: World Meteorological Organization, wmo-no.1076 ed.

Horton, C., M. Clifford, J. Schmitz, and L. H. Kantha. 1997. A real-time oceanographic nowcast/forecast system for the mediterranean sea. J. Geophys. Res. Oceans, *102*(C11), 25123–25156. doi: 10.1029/97JC00533

Hurlburt, H. E. 1986. Dynamic transfer of simulated altimeter data into subsurface information by a numerical ocean model. J. Geophys. Res. *91*(C2), 2372–2400. doi: 10.1029/JC091iC02p02372

Hurlburt, H. E., E. P. Chassignet, J. A. Cummings, A. B. Kara, E. J. Metzger, J. F. Shriver, O. M. Smedstad et al. 2008. Eddy-resolving global ocean prediction, *in* Ocean Modeling in an Eddying Regime, Arlington, VA: Naval Research Laboratory, Oceanography Div., 353–381.

Iovino, D., S. Masina, A. Storto, A. Cipollone, and V. N. Stepanov. 2016. A 1/16 eddying simulation of the global nemo sea-ice–ocean system. Geoscientific Model Development, *9*(8), 2665–2684. doi: 10.5194/gmd-9-2665-2016

Ishiguro, S. 1972. Electronic analogues in oceanography. Oceanogr. Mar. Biol. Annu. Rev., *10*, 27–96.

Janssen, P. A. 1991. Quasi-linear theory of wind-wave generation applied to wave forecasting. J. Phys. Oceanogr., *21*(11), 1631–1642. doi: 10.1175/1520-0485(1991)021<1631:QLTOWW>2.0.CO;2

Janssen, P. A. 2008. Progress in ocean wave forecasting. J. Comput. Physics, *227*(7), 3572–3594. doi: 10.1016/j.jcp.2007.04.029

Jeffreys, H. 1925. On the formation of water waves by wind. Proc. R. Soc. Lond. A, *107*(742), 189–206. doi: 10.1098/rspa.1926.0014

Jelesnianski, C. P. 1965. A numerical calculation of storm tides induced by a tropical storm impinging on a continental self. Mon. Weather Rev, *93*, 343–358. doi: 10.1175/1520-0493(1993)093<0343:ANCOS>2.3.CO;2

Kalman, R. 1963. The theory of optimal control and the calculus of variations, *in* Mathematical Optimization Techniques (R-396-PR), R. Bellman, ed. Santa Monica, CA: Rand Corp., 309–331.

Ko, D. S., P. J. Martin, C. D. Rowley, and R. H. Preller. 2008. A real-time coastal ocean prediction experiment for mrea04. J. Mar. Syst., *69*(1), 17–28. doi: 10.1016/j.jmarsys.2007.02.022

Ko, D., R. Preller, G. Jacobs, T. Tang, and S. Lin. 2003b. Transport reversals at Taiwan strait during october and november 1999. J. Geophys. Res. Oceans, *108*(C11). doi: 10.1029/2003JC001836

Ko, D. S., R. H. Preller, and P. J. Martin. 2003a. An experimental real-time intra americas sea ocean nowcast/forecast system for coastal prediction, *in* Proceedings of AMS 5th Conference on Coastal Atmospheric and Oceanic Prediction and Processes. Hancock County, MS: Stennis Space Center, 97–100.

Komen, G. J., L. Cavaleri, M. Donelan, K. Hasselmann, S. Hasselmann, and P. Janssen. 1996. Dynamics and Modelling of Ocean Waves. Cambridge: Cambridge University Press.

Koshlyakov, M., and Y. Grachev. 1973. Meso-scale currents at a hydrophysical polygon in the tropical Atlantic. Deep-Sea Res Oceanogr. Abstr., *20* (6), 507–526. doi: 10.1016/0011-7471(73)90075-2

Lamb, H. 1932. Hydrodynamics. Cambridge: Cambridge University Press.

Laplace, P. S. 1777. Recherches sur plusieurs points de systeme du monde. In Mémoires de mathématique et de physique. année 1775, p. 91.

Laplace, P. S. 1825. Traité de mécanique céleste, vol. 5. Paris: Crapelet.

Lazzari, P., A. Teruzzi, S. Salon, S. Campagna, C. Calonaci, S. Colella, M. Tonani et al. 2010. Pre-operational short-term forecasts for mediterranean sea biogeochemistry. Ocean Sci., *6*(1), 25–39. doi: 10.5194/os-6-25-2010

Lermusiaux, P. 1999. Estimation and study of mesoscale variability in the strait of sicily. Dyn. Atmos. Oceans, *29*(2), 255–303. doi: 10.1016/S0377-0265(99)00008-1

Lermusiaux, P. 2002. On the mapping of multivariate geophysical fields: Sensitivities to size, scales, and dynamics. J. Atmos. Ocean. Technol., *19* (10), 1602–1637. doi: 10.1175/1520-0426(2002)019<1602:OTMOMG>2.0.CO;2

Lermusiaux, P., P. Haley, W. Leslie, A. Agarwal, O. Logutov, and L. Burton. 2011. Multiscale physical and biological dynamics in the philippine archipelago: Predictions and processes. Oceanography, *24*(1), 70–89. doi: 10.5670/oceanog.2011.05

Lermusiaux, P., and A. Robinson. 2001. Features of dominant mesoscale variability, circulation patterns and dynamics in the strait of sicily. Deep-Sea Res. I: Oceanogr. Res. Pap., *48*(9), 1953–1997. doi: 10.1016/S0967-0637(00)00114-X

Lermusiaux, P., A. Robinson, P. Haley, and W. Leslie. 2002. Advanced interdisciplinary data assimilation: Filtering and smoothing via error subspace statistical estimation, *in* OCEANS'02 MTS/IEEE, vol. 2. Piscataway, NJ: IEEE, 795–802.

Lermusiaux, P. F. 2006. Uncertainty estimation and prediction for interdisciplinary ocean dynamics. J. Comput. Physics, *217*(1), 176–199. doi: 10.1016/j.jcp.2006.02.010

Lermusiaux, P. F. 2007. Adaptive modeling, adaptive data assimilation and adaptive sampling. Physica D, *230*(1), 172–196. doi: 10.1016/j.physd.2007.02.014

Lermusiaux, P. F., P. J. Haley, Jr., and N. K. Yilmaz. 2007. Environmental prediction, path planning and adaptive sampling-sensing and modeling for efficient ocean monitoring, management and pollution control. Sea Technol., *48*(9), 35–38.

Leslie, W., A. Robinson, P. Haley, O. Logutov, P. Moreno, P. Lermusiaux, and E. Coelho. 2008. Verification and training of real-time forecasting of multi-scale ocean dynamics for maritime rapid environmental assessment. J. Mar. Syst., *69*(1), 3–16. doi: 10.1016/j.jmarsys.2007.02.001

Liang, X. S., and A. R. Robinson. 2004. A study of the iceland–faeroe frontal variability using the multiscale energy and vorticity analysis. J. Phys. Oceanogr., *34*(12), 2571–2591. doi: 10.1175/JPO2661.1

Lisitzin, E. 1974. Sea-Level Changes, vol. 8. New York: Elsevier Science.

Logutov, O., and P. Lermusiaux. 2008. Inverse barotropic tidal estimation for regional ocean applications. Ocean Model., *25*(1), 17–34. doi: 10.1016/j.ocemod.2008.06.004

Lorenc, A. C. 1986. Analysis methods for numerical weather prediction. Q. J. R. Meteorol. Soc., *112*(474), 1177–1194.

Lorenc, A. C., S. P. Ballard, R. S. Bell, N. B. Ingleby, P. L. F. Andrews, D. M. Barker, J. R. Bray et al. 2000. The Met. Office global three-dimensional variational data assimilation scheme. Q. J. R. Meteorol. Soc., *126*(570), 2991–3012. doi: 10.1002/qj.49712657002

Lorenz, E. 1982. Atmospheric predictability experiments with a large numerical model. Tellus, *34*(6), 505–513. doi: 10.1111/j.2153-3490.1982.tb01839.x

Lozano, C. J., A. R. Robinson, H. G. Arango, A. Gangopadhyay, Q. Sloan, P. J. Haley, L. Anderson et al. 1996. An interdisciplinary ocean prediction system: Assimilation strategies ana structured data models. Oceanogr. Ser., *61*, 413–452. doi: 10.1016/S0422-9894(96)80018-3

Lubbock, J. 1830. Discussion of tide observations made at liverpool, *in* Abstracts of the Papers Printed in the Philosophical Transactions of the Royal Society of London, vol. 3. London: The Royal Society, 368–368.

Lubbock, J. W. 1836. The bakerian lecture: On the tides at the port of london. Philos. Trans. R. Soc. Lond., *126*, 217–266.

Lynch, D. R., and A. M. Davies. 1995. Quantitative Skill Assessment for Coastal Ocean Models. Washington, D.C.: American Geophysical Union.

Lynch, P. 2008. The eniac forecasts. Bull. Am. Meteorol. Soc., *89* (1), 45.

Manzella, G. M. R., E. Scoccimarro, N. Pinardi, and M. Tonani. 2003. Improved near real-time data management procedures for the mediterranean ocean forecasting system-voluntary observing ship program. Ann. Geophys., *21*(1), 49–62. doi: 10.5194/angeo-21-49-2003

Mason, B. J. 1970. Future developments in meteorology: An outlook to the year 2000. Q. J. R. Meteorol. Soc., *96*(409), 349–368. doi: 10.1002/qj.49709640902

Mason, E., J. Molemaker, A. F. Shchepetkin, F. Colas, J. C. McWilliams, and P. Sangrà. 2010. Procedures for offline grid nesting in regional ocean models. Ocean Model., *35*(1), 1–15. doi: 10.1016/j.ocemod.2010.05.007

McConathy, D. R., and C. C. Kilgus. 1987. The navy geosat mission: an overview. Johns Hopkins APL Tech. Dig., *8*(2), 170–175.

McPhaden, M. J., A. J. Busalacchi, R. Cheney, J.-R. Donguy, K. S. Gage, D. Halpern, M. Ji et al. 1998. The tropical ocean-global atmosphere observing system: A decade of progress. J. Geophys. Res. Oceans, *103*(C7), 14169–14240. doi: 10.1029/97JC02906

McWilliams, J. C. 1976. Maps from the mid-ocean dynamics experiment: Part i. Geostrophic streamfunction. J. Phys. Oceanogr., *6*(6), 810–827.

McWilliams, J. C., and J. M. Restrepo. 1999. The wave-driven ocean circulation. J. Phys. Oceanogr., *29*(10), 2523–2540. doi: 10.1175/1520-0485(1976)006<0810:MFTMOD>2.0.CO;2

Miles, J. W. 1957. On the generation of surface waves by shear flows. J. Fluid Mech., *3*(2), 185–204. doi: 10.1017/S0022112057000567

Miller, R. N., A. R. Robinson, and D. B. Haidvogel. 1983. A baroclinic quasigeostrophic open ocean model. J. Comput. Physics, *50*(1), 38–70. doi: 10.1016/0021-9991(83)90041-4

Miyakoda, K., G. D. Hembree, R. F. Strickler, and I. Shulman. 1972. Cumulative results of extended forecast experiments I. Model performance for winter cases. Mon. Weather Rev., *100*(12), 836–855. doi: 10.1175/1520-0493(1972)100<0836:CROEFE>2.3.CO;2

Miyakoda, K., and A. Rosati. 1977. One-way nested grid models: The interface conditions and the numerical accuracy. Mon. Weather Rev., *105*(9), 1092–1107. doi: 10.1175/1520-0493(1977)105<1092:OWNGMT>2.0.CO;2

Miyakoda, K., J. Smagorinsky, R. F. Strickler, and G. D. Hembree. 1969. Experimental extended predictions with a nine-level hemispheric model. Mon. Weather Rev., *97*(1), 1–76. doi: 10.1175/1520-0493(1969)097<0001:EEPWAN>2.3.CO;2

MODE Group. 1978. The mid-ocean dynamics experiment. Deep Sea Res., *25*(10), 859–910. doi: 10.1016/0146-6291(78)90632-X

Munk, W. 2002. The evolution of physical oceanography in the last hundred years. Oceanography, *15*(1), 135–142. doi: 10.5670/oceanog.2002.45

Munk, W. H., and D. E. Cartwright. 1966. Tidal spectroscopy and prediction. Philos. Trans. R. Soc. Lond. A, *259*(1105), 533–581. doi: 10.1098/rsta.1966.0024

Murphy, A. H. 1998. The early history of probability forecasts: Some extensions and clarifications. Weather Forecast., *13*(1), 5–15.

Murty, T., S. Venkatesh, M. Danard, and M. El-Sabh. 1995. Storm surges in Canadian waters. Atmos. Ocean, *33*(2), 359–387. doi: 10.1080/07055900.1995.9649537

Navarra, A., and V. Simoncini. 2010. *A Guide to Orthogonal Functions for Climate Data Analysis*. New York: Springer Science & Business Media.

Navier, C. 1822. On the laws of motion of fluids taking into consideration the adhesion of the molecules. Ann. Chim. Phys, *19*, 234–245.

Nebeker, F. 1995. Calculating the Weather: Meteorology in the 20th Century, vol. 60. London: Academic Press.

Oddo, P., and N. Pinardi. 2008. Lateral open boundary conditions for nested limited area models: A scale selective approach. Ocean Model., *20*(2), 134–156. doi: 10.1016/j.ocemod.2007.08.001

Oliger, J., and A. Sundström. 1978. Theoretical and practical aspects of some initial boundary value problems in fluid dynamics. SIAM J. Appl. Math., *35*(3), 419–446. doi: 10.1137/0135035

Onken, R., A. R. Robinson, L. Kantha, C. J. Lozano, P. J. Haley, and S. Carniel. 2005. A rapid response nowcast/forecast system using multiply nested ocean models and distributed data systems. J. Mar. Syst., *56*(1), 45–66. doi: 10.1016/j.jmarsys.2004.09.010

Onken, R., A. R. Robinson, P. F. Lermusiaux, P. J. Haley, and L. A. Anderson. 2003. Data-driven simulations of synoptic circulation and transports in the Tunisia-Sardinia-Sicily region. Journal of Geophysical Research: Oceans, *108*(C9). doi: 10.1029/2002JC001348

Osborne, A., and P. M. Rizzoli, eds. 1982a. Dynamics of Ocean Currents and Circulation: Results of POLYMODE and Related Investigations. Topics in Ocean Physics, Societa' italiana di Fisica. New York: Elsevier.

Osborne, A., and P. M. Rizzoli, eds. 1982b. Dynamics of Ocean Currents and Circulation: Results of POLYMODE and Related Investigations, vol. Topics in Ocean Physics. New York: Elsevier.

Palmer, T., and R. Hagedorn. 2006. Predictability of Weather and Climate. Cambridge: Cambridge University Press.

Peloquin, R. 1992. The Navy ocean modeling and prediction program—From research to operations: An overview. Oceanography, *5*(1), 4–8. doi: 10.5670/oceanog.1992.25

Philander, S. G. 1989. El Niño, La Niña, and the Southern Oscillation, vol. 46. London: Academic press.

Phillips, N. A. 1951. A simple three-dimensional model for the study of large-scale extratropical flow patterns. J. Meteorol., *8*(6), 381–394. doi: 10.1175/1520

Phillips, O. M. 1957. On the generation of waves by turbulent wind. J. Fluid Mech, *2*(5), 417–445.

Pierson, W. J., and W. Marks. 1952. The power spectrum analysis of ocean-wave records. Eos Trans. AGU, *33*(6), 834–844. doi: 10.1029/TR033i006p00834

Pinardi, N., I. Allen, E. Demirov, P. De Mey, G. Korres, A. Lascaratos, P.-Y. Le Traon, et al. 2003. The mediterranean ocean forecasting system: First phase of implementation (1998–2001). Ann. Geophysicae, *21*(1), 3–20. doi: 10.5194/angeo-21-3-2003

Pinardi, N., A. Bonazzi, S. Dobricic, R. F. Milliff, C. K. Wikle, and L. M. Berliner. 2011. Ocean ensemble forecasting. Part ii: Mediterranean forecast system response. Q. J. R. Meteorol. Soc., *137*(657), 879–893. doi: 10.1002/qj.816

Pinardi, N., and G. Coppini. 2010. Preface "Operational oceanography in the mediterranean sea: the second stage of development." Ocean Sci., *6*(1), 263–267. doi: 10.5194/os-6-263-2010

Pinardi, N., and N. Flemming. 1998. The mediterranean forecasting system science plan. Tech. Rep., 11, EuroGOOS. Southampton, UK: EuroGOOS Office.

Pinardi, N., G. Korres, A. Lascaratos, V. Roussenov, and E. Stanev. 1997. Numerical simulation of the interannual variability of the mediterranean sea upper ocean circulation. Geophys. Res. Lett., *24*(4), 425–428.

Pinardi, N., and A. R. Robinson. 1986. Quasigeostrophic energetics of open ocean regions. Dyn. Atmos. Oceans, *10*(3), 185–219. doi: 10.1016/0377-0265(86)90013-8

Pinardi, N., and A. R. Robinson. 1987. Dynamics of deep thermocline jets in the polymode region. J. Phys. Oceanogr., *17*(8), 1163–1188. doi: 10.1175/1520-0485(1987)017<1163:DODTJI>2.0.CO;2

Pinardi, N., and J. Woods. 2002. Ocean Forecasting: Conceptual Basis and Applications. New York: Springer Science & Business Media.

Plag, H.-P. 2008. Geo, geoss and igos-p: The framework of global earth observations, *in* Proceedings of IGS 2006 Workshop, Darmstadt. Geneva: GEO (Group on Earth Observations).

Platzman, G. W. 1979. The eniac computations of 1950—gateway to numerical weather prediction. Bull. Am. Meteorol. Soc., *60* (4), 302–312. doi: 10.1175/1520

Poincare, H. 1910. Lecons de mecanique celeste, vol. 3: Theorie des marees. Paris: Gauthler-Villars, 16.

Prandle, D., and J. Wolf. 1978. The interaction of surge and tide in the North Sea and River Thames. Geophys. J. Int., *55*(1), 203–216. doi: 10.1111/j.1365-246X.1978.tb04758.x

Preller, R. H. 1992. Sea ice prediction: The development of a suite of sea-ice forecasting systems for the northern hemisphere. Oceanography, *5*(1), 64–68. doi: 10.5670/oceanog.1992.35

Proudman, J. 1917. On the dynamic equation of the tides. Parts 1–3. Proc. London Math. Soc., *2*(18), 1–68.

Proudman, J. 1929. The effects on the sea of changes in atmospheric pressure. Geophys. J. Int., *2*(s4), 197–209. doi: 10.1111/j.1365-246X.1929.tb05408.x

Pugh, D., and P. Woodworth. 2014. Sea-Level Science: Understanding Tides, Surges, Tsunamis and Mean Sea-Level Changes. Cambridge: Cambridge University Press.

Ramp, S. R., P. F. Lermusiaux, I. Shulman, Y. Chao, R. E. Wolf, and F. L. Bahr. 2011. Oceanographic and atmospheric conditions on the continental shelf north of the monterey bay during august 2006. Dyn. Atmos. Oceans, *52*(1), 192–223. doi: 10.1016/j.dynatmoce.2011.04.005

Reid, R. O., and B. R. Bodine. 1968. Numerical model for storm surges in galveston bay. J. Waterw. Harbors Div., *94* (1), 33–58.

Rhodes, R. C., H. E. Hurlburt, A. J. Wallcraft, C. N. Barron, P. J. Martin, E. J. Metzger, J. F. Shriver, et al. 2002. Navy real-time global modeling systems. Oceanography, *15*(1), 29–43.

Richardson, L. F. 1922. Weather Prediction by Numerical Process. Cambridge University Press, Cambridge, UK. Reprinted by Dover, New York, 1965. Second edn., 2007, Cambridge University Press, with a new foreword by Peter Lynch edition.

Robinson, A. R. 1983. Overview and summary of eddy science, *in Eddies in Marine Science*, Springer, Berlin, Heidelberg, 3–15.

Robinson, A. R. 1992. Shipboard prediction with a regional forecast model. Oceanography, *5*(1), 42. doi: 10.5670/oceanog.1992.31

Robinson, A. R., H. G. Arango, W. G. Leslie, A. J. Miller, A. Warn-Varnas, and P.-M. Poulain. 1996. Real-time operational forecasting on shipboard of the iceland-faeroe frontal variability. Bull. Am. Meteorol. Soc., *77* (2), 243–259. doi: 10.1175/1520

Robinson, A. R., J. A. Carton, N. Pinardi, and C. N. Mooers. 1986. Dynamical forecasting and dynamical interpolation: An experiment in the california current. J. Phys. Oceanogr., *16*(9), 1561–1579. doi: 10.1175/1520-0485(1986)016<1561:DFADIA>2.0.CO;2

Robinson, A., J. Carton, C. Mooers, L. Walstad, E. Carter, M. Rienecker, J. Smith et al. 1984. A real-time dynamical forecast of ocean synoptic/mesoscale eddies. Nature, *309*, 781–783. doi: 10.1038/309781a0

Robinson, A. R., S. M. Glenn, M. A. Spall, L. J. Walstad, G. M. Gardner, and W. G. Leslie. 1989. Forecasting gulf stream meanders and rings. Eos Trans. AGU, *70* (45), 1464–1473. doi: 10.1029/89EO00346

Robinson, A., and D. Haidvogel. 1980. Dynamical forecast experiments with a barotropic open ocean model. J. Phys. Oceanogr., *10*(12), 1909–1928. doi: 10.1175/1520-0485(1980)010<1909:DFEWAB>2.0.CO;2

Robinson, A., P. Haley, P. Lermusiaux, and W. Leslie. 2002. Predictive skill, predictive capability and predictability in ocean forecasting, *in* OCEANS'02 MTS/IEEE, vol. 2, Piscataway, NJ: IEEE, 787–794.

Robinson, A. R., and W. G. Leslie. 1985. Estimation and prediction of oceanic eddy fields. Progr. Oceanogr., *14*, 485–510. doi: 10.1016/0079-6611(85)90024-2

Robinson, A., and J. Sellschopp. 2002. Rapid assessment of the coastal ocean environment, *in* Ocean Forecasting: Conceptual Basis and Applications. N. Pinardi and J. Woods, eds., New York: Springer Science & Business Media.

Robinson, A. R., M. A. Spall, and N. Pinardi. 1988. Gulf stream simulations and the dynamics of ring and meander processes. J. Phys. Oceanogr., *18*(12), 1811–1854. doi: 10.1175/1520-0485(1988)018<1811:GSSATD>2.0.CO;2

Robinson, A., J. Sellschopp, A. Warn-Varnas, W. Leslie, C. Lozano, P. Haley, L. Anderson et al. 1999. The Atlantic ionian stream. J. Mar. Syst., *20*(1), 129–156. doi: 10.1016/S0924-7963(98)00079-7

Robinson, A., J. Sellschopp, W. Leslie, A. Alvarez, G. Baldasserini, P. Haley, Jr., P. Lermusiaux et al. 2002. Forecasting synoptic transients in the eastern ligurian sea. HARVARD UNIV CAMBRIDGE MA, DEPT OF EARTH AND PLANETARY SCIENCES.

Robinson, A., A. Tomasin, and A. Artegiani. 1973. Flooding of venice: Phenomenology and prediction of the adriatic storm surge. Q. J. R. Meteorol. Soc., *99*(422), 688–692. doi: 10.1002/qj.49709942210

Robinson, A. R., and L. J. Walstad. 1987. The harvard open ocean model: Calibration and application to dynamical process, forecasting, and data assimilation studies. App. Numer. Math., *3*(1-2), 89–131. doi: 10.1016/0168-9274(87)90008-0

Rodgers, C. D. 2000. Inverse Methods for Atmospheric Sounding: Theory and Practice, vol. 2. Singapore: World scientific.

Rogers, W. E., Dykes, J. D., and P. A. Wittmann. 2014. US Navy global and regional wave modeling. Oceanography, *27*(3), 56–67.

Rosati, A., and K. Miyakoda. 1988. A general circulation model for upper ocean simulation. J. Phys. Oceanogr., *18*(11), 1601–1626. doi: 10.1175/1520-0485

Rossiter, J. 1954. The North Sea storm surge of 31 january and 1 february 1953. Philos. Trans. R. Soc., A, *246*(915), 371–400. doi: 10.1098/rsta.1954.0002

Saha, S., S. Moorthi, X. Wu, J. Wang, S. Nadiga, P. Tripp et al. 2014. The ncep climate forecast system ver. 2. J. Clim., *27*(6), 2185–2208. doi: 10.1175/JCLI-D-12-00823.1

Schiller, A., and N. Smith. 2006. Bluelink: Large-to-coastal scale operational oceanography in the southern hemisphere, *in* Ocean Weather Forecasting. New York: Springer, 427–439.

Shapiro, R. 1971. The use of linear filtering as a parameterization of atmospheric diffusion. J. Atmos. Sci., *28*(4), 523–531. doi: 10.1175/1520-0469(1971)028<0523:TUOLFA>2.0.CO;2

Snodgrass, F., G. W. Groves, K. Hasselmann, G. Miller, W. Munk, and W. Powers. 1966. Propagation of ocean swell across the pacific. Philos. Trans. R. Soc. Lond. A, *259*(1103), 431–497. doi: 10.1098/rsta.1966.0022

Sorenson, H. W. 1970. Least-squares estimation: From Gauss to Kalman. IEEE Spectrum, *7*(7), 63–68. doi: 10.1109/MSPEC.1970.5213471

Spall, M. A. 1989. Regional primitive equation modeling and analysis of the polymode data set. Dyn. Atmos. Oceans, *14*, 125–174. doi: 10.1016/0377-0265(89)90060-2

Spall, M. A., and W. R. Holland. 1991. A nested primitive equation model for oceanic applications. J. Phys. Oceanogr., *21*(2), 205–220. doi: 10.1175/1520

Spall, M. A., and A. R. Robinson. 1989. A new open ocean, hybrid coordinate primitive equation model. Math. Comput. Simul., *31*(3), 241–269. doi: 10.1016/0378-4754(89)90162-6

Stammer, D., R. Ray, O. B. Andersen, B. Arbic, W. Bosch, L. Carrère, Y. Cheng et al. 2014. Accuracy assessment of global barotropic ocean tide models. Rev. Geophys., *52*(3), 243–282. doi: 10.1002/2014RG000450

Stokes, G. G. 1848. On the steady motion of incompressible fluids. Transactions of the Cambridge Philosophical Society, 7, 439.

Storto, A., S. Dobricic, S. Masina, and P. Di Pietro. 2011. Assimilating along-track altimetric observations through local hydrostatic adjustment in a global ocean variational assimilation system. Mon. Weather Rev., *139*(3), 738–754. doi: 10.1175/2010MWR3350.1

Summerhayes, C. 2002. The global ocean observing system (GOOS) in 1998, *in* Operational Oceanography Implementation at the European and Regional Scales, vol. 66, N. Fiemming, S. Vallerga, N. Pinardi, H. Behrens, G. Manzella, and D. Prandle, eds., 57–66. Elsevier Oceanography Series, The Netherlands, doi: 0.1016/S0422-9894(02)80010-1

Sverdrup, H., M. Johnson, and R. Fleming. 1942. The Oceans, vols. I and II. Upper Saddle River, NJ: Prentice-Hall, Inc.

Sverdrup, H. U., and W. H. Munk. 1947. Wind, sea, and swell: Theory of relations for forecasting. Tec. Rep. H.O. Pub. No. 601. Blythe, CA: US Hydrographic Office.

Sztobryn, M. 2003. Forecast of storm surge by means of artificial neural network. J. Sea Res., *49*(4), 317–322. doi: 10.1016/S1385-1101(03)00024-8

Talagrand, O. 2003. Variational assimilation. adjoint equations, *in* Data Assimilation for the Earth System, New York: Springer, 37–53.

Temam, R., and J. Tribbia. 2003. Open boundary conditions for the primitive and Boussinesq equations. J. Atmos. Sci., *60*(21), 2647–2660. doi: 10.1175/1520-0469(2003)060<2647:OBCFTP> 2.0.CO;2

Thomson, W. 1880. 1. On gravitational oscillations of rotating water. Proc. R. Soc. Edinb. *10*, 92–100. doi: 10.1080/14786448008626897

Tolman, H. L. 1997. User manual and system documentation of WAVEWATCH-iii version 1.15. Tech. Note, *16*. Camp Springs, MD: U.S. Dept. of Commerce.

Tonani, M., M. Balmaseda, L. Bertino, E. Blockley, G. Brassington, F. Davidson, Y. Drillet et al. 2015. Status and future of global and regional ocean prediction systems. J. Oper. Oceanogr., *8*, 201–220. doi: 10.1080/1755876X.2015.1049892

Trotta, F., E. Fenu, N. Pinardi, D. Bruciaferri, L. Giacomelli, I. Federico, and G. Coppini. 2016. A structured and unstructured grid relocatable ocean platform for forecasting (SURF). Deep-Sea Res. II Topic. Stud. Oceanogr., *133*, 54–75. doi: 10.1016/j.dsr2.2016.05.004

Tsimplis, M. 1997. Tides and sea-level variability at the strait of euripus. Estuar. Coast. Shelf Sci., *44*(1), 91–101. doi: 10.1006/ecss.1996.0128

Uppala, S., A. Hollingsworth, S. Tibaldi, and P. Kallberg. 1984. Results from two recent observing system experiments at ecmwf, *in* Proceedings of the ECMWF Seminar/Workshop on Data Assimilation Systems and Observing System Experiments, vol. 1, Sheffield Park, Reading, UK: ECMWF, 165–202.

Vichi, M., N. Pinardi, and S. Masina. 2007. A generalized model of pelagic biogeochemistry for the global ocean ecosystem. Part i: Theory. J. Mar. Syst., *64*(1), 89–109. doi: 10.1016/j.jmarsys.2006.03.006

WAM Group. 1988. The wam model—A third generation ocean wave prediction model. J. Phys. Oceanogr., *18*(12), 1775–1810. doi: 10.1175/1520-0485(1988)018<1775:TWMTGO>2.0.CO;2

Wang, H.-H., and P. Halpern. 1970. Experiments with a regional fine-mesh prediction model. J. Appl. Meteorol., *9*(4), 545–553. doi: 10.1175/1520-0450(1970)009<0545:EWARFM>2.0.CO;2

Waseda, T., Y. Toba, and M. P. Tulin. 2001. Adjustment of wind waves to sudden changes of wind speed. J. Oceanogr., *57*(5), 519–533. doi: 10.1023/A:1021287032271

Wei, M., G. Jacobs, C. Rowley, C. N. Barron, P. Hogan, P. Spence, O. M. Smedstad et al. 2016. The performance of the U.S. Navy's RELO ensemble, NCOM, HYCOM during the period of GLAD at-sea experiment in the Gulf of Mexico. Deep-Sea Res. II: Topic. Stud. Oceanogr., *129*, 374–393. doi: 10.1016/j.dsr2.2013.09.002

Weisse, R., D. Bellafiore, M. Menéndez, F. Méndez, R. J. Nicholls, G. Umgiesser, and P. Willems. 2014. Changing extreme sea levels along European coasts. Coast. Eng., *87*, 4–14. doi: 10.1016/j.coastaleng.2013.10.017

Whewell, W. 1833. Essay towards a first approximation to a map of cotidal lines. Philos. Trans. R. Soc. Lond., *123*, 147–236.

Wilson, C., K. J. Horsburgh, J. Williams, J. Flowerdew, and L. Zanna. 2013. Tide-surge adjoint modeling: A new technique to understand forecast uncertainty. J. Geophys. Res. Oceans, *118*(10), 5092–5108. doi: 10.1002/jgrc.20364

Woods, A. 2006. 1794 to 1980: The Formative Years. New York: Springer, 72–84. ISBN 978-0-387-26929-0.

Wunsch, C. 2002. Ocean observations and the climate forecast problem. Int. Geophys., *83*, 233 – 245. doi: 10.1016/S0074-6142(02)80170-X

Yeh, G.-T., and F.-K. Chou. 1979. Moving boundary numerical surge model. J. Waterw., Port Coast. Ocean Div., *105*(3), 247–263.

Young, T. 1813. A theory of tides, including the consideration of resistance. Nicholson J., also in Young [1855], *2*, 262–390.

Zebiak, S. E., and M. A. Cane. 1987. A model El Niño–Southern oscillation. Mon. Weather Rev., *115*(10), 2262–2278.

Zijl, F., M. Verlaan, and H. Gerritsen. 2013. Improved water-level forecasting for the northwest european shelf and North Sea through direct modelling of tide, surge and non-linear interaction. Ocean Dyn., *63*(7), 823–847. doi: 10.1007/s10236-013-0624-2

Received: *6 March 2017*; revised: *24 May 2017*.

*Editor's note*: Contributions to *The Sea: The Science of Ocean Prediction* are being published separately in special issues of *Journal of Marine Research* and will be made available in a forthcoming supplement as Volume 17 of the series.